Biomaterials 293 (2023) 121982

Contents lists available at ScienceDirect

Biomaterials

journal homepage: www.elsevier.com/locate/biomaterials

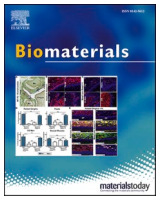

RGD density along with substrate stiffness regulate hPSC hepatocyte functionality through YAP signalling

Samuel J.I. Blackford [a,b,c,d,*], Tracy T.L. Yu [b], Michael D.A. Norman [b], Adam M. Syanda [a,d], Michail Manolakakis [e,f], Dariusz Lachowski [g], Ziqian Yan [b], Yunzhe Guo [b], Elena Garitta [a,d], Federica Riccio [c], Geraldine M. Jowett [b,c], Soon Seng Ng [a,d], Santiago Vernia [e,f], Armando E. del Río Hernández [g], Eileen Gentleman [b,**,1], S. Tamir Rashid [a,d,***,1]

[a] Department of Metabolism, Digestion and Reproduction, Imperial College London, UK
[b] Centre for Craniofacial & Regenerative Biology, King's College London, UK
[c] Centre for Gene Therapy & Regenerative Medicine, King's College London, UK
[d] NIHR Imperial BRC iPSC and Organoid Core Facility, Imperial College London, UK
[e] MRC London Institute of Medical Sciences, UK
[f] Institute of Clinical Sciences, Imperial College London, UK
[g] Cellular and Molecular Biomechanics Laboratory, Department of Bioengineering, Imperial College London, UK

ARTICLE INFO

Keywords:
Hydrogel
Hepatocyte
Induced pluripotent stem cell
Mechanosensing
YAP

ABSTRACT

Human pluripotent stem cell-derived hepatocytes (hPSC-Heps) may be suitable for treating liver diseases, but differentiation protocols often fail to yield adult-like cells. We hypothesised that replicating healthy liver niche biochemical and biophysical cues would produce hepatocytes with desired metabolic functionality. Using 2D synthetic hydrogels which independently control mechanical properties and biochemical cues, we found that culturing hPSC-Heps on surfaces matching the stiffness of fibrotic liver tissue upregulated expression of genes for RGD-binding integrins, and increased expression of *YAP/TAZ* and their transcriptional targets. Alternatively, culture on soft, healthy liver-like substrates drove increases in cytochrome p450 activity and ureagenesis. Knockdown of *ITGB1* or reducing RGD-motif-containing peptide concentration in stiff hydrogels reduced YAP activity and improved metabolic functionality; however, on soft substrates, reducing RGD concentration had the opposite effect. Furthermore, targeting YAP activity with verteporfin or forskolin increased cytochrome p450 activity, with forskolin dramatically enhancing urea synthesis. hPSC-Heps could also be successfully encapsulated within RGD peptide-containing hydrogels without negatively impacting hepatic functionality, and compared to 2D cultures, 3D cultured hPSC-Heps secreted significantly less fetal liver-associated alpha-fetoprotein, suggesting furthered differentiation. Our platform overcomes technical hurdles in replicating the liver niche, and allowed us to identify a role for YAP/TAZ-mediated mechanosensing in hPSC-Hep differentiation.

1. Introduction

Over 600 million people worldwide are affected by one of the many diseases that afflict the liver, and more than 1 million die of chronic or acute liver failure every year [1]. Many genetic and metabolic diseases impact the liver, driving fibrosis and cirrhosis, but the only curative intervention for end-stage liver disease is orthotopic liver transplantation. Transplantation of hepatocytes alone could be an effective alternative to whole organ transplantation [2]. However, primary human hepatocytes (PHH) derived from donor organs are unable to meet the demand for cell therapies.

Human pluripotent stem cell-derived hepatocytes (hPSC-Heps) may be an effective alternative for PHH-based cell therapies; however, protocols to generate hPSC-Heps produce cells with either hybrid features

* Corresponding author. Department of Metabolism, Digestion and Reproduction, Imperial College London, UK.
** Corresponding author. Centre for Craniofacial & Regenerative Biology, King's College London, UK
*** Corresponding author. Department of Metabolism, Digestion and Reproduction, Imperial College London, UK.
E-mail addresses: sji.blackford@outlook.com (S.J.I. Blackford), eileen.gentleman@kcl.ac.uk (E. Gentleman), t.rashid@imperial.ac.uk (S.T. Rashid).
[1] These authors contributed equally to this work.

https://doi.org/10.1016/j.biomaterials.2022.121982
Received 16 January 2022; Received in revised form 13 December 2022; Accepted 22 December 2022
Available online 22 December 2022

of hepatic, intestinal, fibroblastic, and pluripotent cells [3], or are similar to fetal hepatocytes [4]. Bridging the functional gap between hPSC-Heps and PHHs will likely require correctly replicating the cell's niche, as extrinsic biological stimuli in the native liver are known to regulate normal hepatocyte function. As a result, extracellular matrix (ECM) interactions [5], multicellularity [6], and paracrine signals [7], have been all explored to improve hPSC-Heps' functional equivalence to PHH.

In addition to the biological components of the niche, in vivo evidence suggests that changes in the liver's physical properties impact hepatocytes. Indeed, liver stiffness is used to diagnose liver malfunction, as fibrosis results in increased tissue Young's modulus (*E*). Increased tissue stiffness is also associated with hepatocellular carcinoma (HCC), which is regulated by beta-1 integrins [8], and inhibition of beta-1 integrin signalling may prevent liver malfunction and the development of HCC [9,10]. Yes-associated protein (YAP) and transcription coactivator with PDZ-binding motif (TAZ) are mechanosensitive nuclear effectors of the Hippo signalling pathway. During fibrosis, ECM stiffening enhances YAP activation [11], and in non-human primates with liver fibrosis, YAP localises within the nucleus of hepatocytes and correlates with increased transforming growth factor-beta (TGFβ) expression [12]. Moreover, loss of Lats1/2, the direct upstream regulators of YAP/TAZ, forces a hepatoblast to cholangiocyte fate commitment [13], and activation of YAP in adult hepatocytes causes dedifferentiation [14].

Hepatocytes isolated from fibrotic end-stage disease livers have significantly reduced expression of Hepatocyte Nuclear Factor-4-Alpha (HNF4α) and produce significantly less albumin and urea compared to normal hepatocytes. Strikingly, hepatocytes isolated from diseased livers can recover their mature phenotype once transplanted back into a heathy non-cirrhotic microenvironment [15]. Taken together, these observations suggest that hepatocyte function may be regulated by tissue stiffness and is likely dependent on YAP/TAZ signalling. Furthermore, they suggest that placing hepatocytes in tissue-like mechanical environments can prompt them to adopt normal phenotypes. In addition to stiffness, other cues from the matrix may also influence hPSC-Heps. For example, rat hepatocytes are responsive to substrate-bound fibronectin. As fibronectin density increases, the level of liver-specific functional activity decreases [16].

The RGD tripeptide, originally identified as the integrin binding sequence within fibronectin, interacts with αvβ3, α5β1, and αIIbβ3 integrins [17], and hydrogels incorporating RGD better support the viability and function of PHH than scaffolds lacking RGD or Matrigel [18]. Moreover, primary rat hepatocytes cultured in the presence of increasing concentrations of RGD peptide showed enhanced beta-1-integrin signalling [19]. However, decoupling the impact of stiffness from ligand concentration is challenging. Recent studies have begun to dissect how liver niche mechanics influence the function of both hepatic cell lines and rodent hepatocytes [20–23]; however, results are often muddled by culture conditions relying on fetal bovine serum (FBS), which is known to impact YAP activity [24]. Moreover, the ECM is a complex network of proteins and polysaccharide chains, whereas the RGD adhesive peptide presents the minimal recognition sequence required for cell adhesion [25].

Here, we took a reductionist approach to investigate the impact of stiffness on the differentiation of hPSC-Heps within fully defined serum-free media. We created poly (ethylene) glycol (PEG) hydrogels, which allow for precise control over stiffness, independently of ligand density [26]. Our hydrogels allowed for successful culture of hPSC-Heps on defined substrates in the absence of ROCK inhibitor. When matured on soft, normal liver-like substrates, hPSC-Heps show reduced YAP activity and acquired an advanced hepatic phenotype compared to those cultured on stiff fibrotic liver-like substrates, independently from changes to *HNF4A* gene expression. Additionally, through *ITGB1* knockdown or by reducing the concentration of RGD, we show reduced YAP activity and improved hepatocyte differentiation, even on stiff hydrogels, suggesting a link between hPSC-Heps' ability to sense stiffness and adhesive ligand concentration via beta-1 integrins. We also show that hPSC-Heps can be successfully encapsulated within PEG hydrogels to enable 3D maturation and mechanosensing. Our platform overcomes challenges associated with many synthetic and hybrid materials for studying hepatic mechanosensing [27–29] and allowed us to tease apart the influences of stiffness and ligand density on hPSC-Heps differentiation and YAP/TAZ activity.

2. Materials and methods

2.1. PEG-Peptide Conjugation

Custom-designed peptides (Peptide Protein Research Ltd, Southampton, UK) (>98% purity) were used to create PEG-peptide conjugates. Adhesive peptides presenting RGD in a looped configuration ((RGDSGD)K-GDQGIAGF-ERC-NH2) or non-adhesive sequences (Ac-KDW-ERC-NH2) were conjugated to 4-arm PEG activated at each terminus with nitrophenyl carbonate (PEG-4NPC) (JenKem Technology, Plano, TX). To create PEG-peptide conjugates, peptide was dissolved in anhydrous dimethyl sulfoxide (DMSO) (Sigma-Aldrich, St. Louis, MO) at 10 mg/ml, and anhydrous triethylamine (Sigma-Aldrich, St. Louis, MO) was added stoichiometrically to convert the peptide salts into their free forms to deprotonate the primary amine from the lysine side chain. Next, a 16.67 mg/ml solution of 10 kDa PEG-4NPC in DMSO was reacted with peptides on an orbital shaker at either an 8:1 ratio of excess peptide to PEG-4NPC at room temperature (RT) for 2 h (adhesive peptide), or a 12:1 ratio at RT for 0.5 h (non-adhesive peptide). Conjugation occurred through a nucleophilic substitution reaction between the primary amine on the side chain of the lysine residue of each peptide and NPC esters forming stable carbamate linkages.

PEG-peptide conjugates were snap frozen on dry ice and lyophilised. To reduce disulfide bonds, conjugates were dissolved in sodium carbonate-bicarbonate buffer at pH 9.0 and treated with 1,4-Dithiothreitol (DTT) (0.1 g/ml) for 3 h at RT after argon purging (molar ratio of 8:1, DTT:peptide). PEG-peptide-conjugates were then purified in Milli-Q water 5 times using 10 kDa cut-off Amicon Ultra-15 Centrifugal Filter Units (Merck Millipore, Burlington, MA), snap frozen on dry ice, and lyophilised again prior to storage at −20 °C.

2.2. PEG Hydrogel Fabrication

Hydrogels were formed by reacting PEG-peptide conjugates with 20 kDa star-shaped 4-arm PEG that presents vinyl sulfone (VS) groups at each chain terminus (PEG-4VS). The reaction was performed in a stoichiometric ratio of 1:1 in 20 mM HEPES buffer (pH 8.1, with 1X HBSS; final volume 55 μl) through a Michael-type reaction between a cysteine thiol on the C-terminal of the peptide with the VS group on PEG-4VS. Directly after the onset of this reaction, 50 μl of vortexed pre-hydrogel solution was transferred into the centre of a 6-well plate well and covered by a Sigmacote-treated (Sigma-Aldrich, St. Louis, MO) 25 mm diameter circular glass cover slip. Hydrogels were allowed to form at 37 °C for 1 h prior to the addition of HepatoZYME-SFM and the removal of the glass coverslip. Hydrogels were formed with polymer concentrations of 2.5 and 10% (w/v). The concentration of adhesive PEG-peptide conjugates was maintained at 1770 μM; apart from experiments evaluating RGD concentration - where hydrogels containing either 1770 or 885 μM of adhesive PEG-peptide conjugates were used. Hydrogels were then stored at 4 °C for 24 h before cell seeding.

2.3. Atomic Force Microscopy Force Spectroscopy Measurements

30 μl hydrogels were formed in Sigmacote-treated 6-mm-diameter glass cylindrical moulds in 35-mm petri dishes and stored in PBS at 4 °C. Force-distance measurements were carried out on a JPK NanoWizard 4 (JPK Instruments, Berlin, Germany) directly on hydrogels immersed in PBS at RT, as previously described [30]. Spherical glass beads (diameter

10 μm; Whitehouse Scientific, Chester, UK) were mounted on tipless triangular silicon nitride cantilevers (spring constant (K) ≈ 0.12 N m^{-1}; Bruker AFM Probes, Camarillo, CA) using ultraviolet-crosslinked Loctite superglue. The deflection sensitivity of the AFM photodiode was calibrated by collecting a single force-distance curve on a glass slide. Cantilevers were calibrated using the thermal method [31] in air.

Measurements were made at 6 locations across hydrogels' surfaces (100 μm × 100 μm areas, 100 force curves per location on 3 hydrogels per condition). Indentations were carried out with a relative setpoint force of 3 nN and a loading rate of 4 μm s^{-1}. Data were collected using JPK proprietary SPM software (version 6.1, JPK Instruments, Berlin, Germany). The Oliver–Pharr model for a spherical tip was used to determine E. Outliers were removed using a ROUT test (Q = 1%). We assumed that volume was conserved and assigned a Poisson's ratio of 0.5.

2.4. Cell Culture

Two cGMP hiPSC lines (CGT-RCiB-10 [line 1; Cell & Gene Therapy Catapult, London, U.K.] and LiPSC-GR1.1 [line 2; Lonza, Walkersville, MD]), one cGMP hESC line (KCL037 [line 3; Gifted from D. Ilic, King's College London]) and one GFP + ve hiPSC line (AICS-12 mEGFP a-tubulin [Line 4; Allen Institute for Cell Science, Seattle, WA]) were used in this study. Lines were maintained on Vitronectin XF (STEMCELL Technologies, Vancouver, BC, Canada) coated Corning Costar TC-treated 6-well plates (Sigma–Aldrich, St. Louis, MO) in TeSR-E8 (STEMCELL Technologies, Vancouver, BC, Canada) and passaged every 4 days using Gentle Cell Dissociation Reagent (STEMCELL Technologies). Line 3 was passaged in TeSR-8 supplemented with 10 μM Y-27632 dihydrochloride (R&D Systems, Minneapolis, MN) to ensure cell survival.

Hepatocyte differentiation was carried out as previously described [32] in Essential 6 Medium (Thermo Fisher Scientific, Waltham, MA; days 1–2), RPMI-1640 Medium (Sigma–Aldrich; days 3–8) and HepatoZYME-SFM (Thermo Fisher Scientific; day 9 onward) within Corning Falcon 100 × 20 mm style tissue culture dishes (Sigma-Aldrich). The following growth factors and small molecules were supplemented into the media for hepatocyte differentiation: 3 μM CHIR9901 [Day 1] (Sigma-Aldrich), 10 ng/ml BMP4 [Day 1–2] (R&D Systems), 10 μM LY29004 [Day 1–2] (Promega, Madison, WI), 80 ng/ml FGF2 [Day 1–3] (R&D Systems), 100 ng/ml [Day 1–3] and 50 ng/ml [Day 4–8] Activin A (Qkine, Cambridge, U.K.), 10 ng/ml oncostatin M (OSM) [Day 9 onwards] (R&D Systems) and 50 ng/ml hepatocyte growth factor (HGF) [Day 9 onwards] (PeproTech, Rocky Hill, NJ). Day 14 hPSC-derived hepatic endoderm was dissociated into a single-cell suspension using TrypLE Express Enzyme (1 ×), no phenol red (Thermo Fisher Scientific).

Additional small molecules were used at the following concentrations: 10 μM Forskolin (APExBIO Technology, Houston, TX), 1 μM Latrunculin A (Cayman Chemical, Ann Arbor, MI), 0.35 μM Verteporfin (Selleck Chemicals, Houston, TX), and 5 μM Y-27632 (R&D Systems, Minneapolis, MN).

Gene knockdown by siRNA transfection was performed as previously described [33]. siRNAs (SMARTpool) were purchased from Dharmacon (Lafayette, CO) and transfected at 100 nM with Lipofectamine RNAiMAX in Opti-MEM (Thermo Fisher Scientific) overnight.

2.5. Cell Seeding onto 2D Hydrogels

hPSC-derived hepatic endoderm stage cells after 14 days of differentiation were dissociated to single cells after a 15 min treatment with TrypLE Express Enzyme (1X), No Phenol Red. Automated cell counting (NucleoCounter NC-200: ChemoMetec A/S, Lillerød, Denmark) was performed and cells were resuspended in fresh fully supplemented HepatoZYME-SFM. A 300 μl volume containing 0.6 × 10^6 cells was seeded directly onto the middle region of the 2D hydrogel. After 10 min, hydrogels were transferred to a 37 °C incubator and cells were left 6 h to adhere. 2 ml of fully supplemented HepatoZYME-SFM was then added to the hydrogel cultures. Media was subsequently refreshed every 48 h.

2.6. 3D Cell Encapsulation

Sigmacote siliconised, 10 mm-diameter glass cylindrical moulds were placed in pre-warmed 24-well plates. Hepatic endoderm stage cells were mixed within pre-hydrogel solution at a concentration of 4 × 10^6 cells/ml. The hydrogel fabrication reaction for 3D encapsulation occurred within a 20 mM HEPES buffer (pH 8.0, 1X HBSS). The same 2.5 and 10% PEG concentrations were used, with 1770 μM adhesive peptide. The reaction was stopped after 35 min by the addition of cell culture media, and the glass mould removed. Culture media was refreshed every 48 h.

Alginate encapsulations were carried out as previously described [32]. In brief, spheroids were washed in saline before being resuspended into a final 1.8% ultra-pure low-viscosity, high-glucuronic acid (≥60%), sodium alginate (FMC BioPolymer, Drammen, Norway) solution, which was then delivered by syringe pump through a 0.2 mm diameter nozzle, from which droplets were electrostatically deposited into a divalent cationic solution (1 mM $BaCl_2$ + 50 mM $CaCl_2$) to cause gelation.

2.7. Brightfield and Immunofluorescence Imaging

Brightfield microscopy was performed on a Leica DMIL LED inverted microscope and imaged using the Leica DFC3000 G camera (Leica Microsystems, Wetzlar, Germany).

Samples were fixed for 10 min with 4% w/v paraformaldehyde. Except for albumin staining, cells were permeabilised with 0.1% Triton X-100 (Sigma-Aldrich) and then blocked in 1% w/v bovine serum albumin (Sigma-Aldrich) and 22.52 mg/ml glycine (Sigma-Aldrich). Cells were incubated with primary antibodies in blocking solution overnight at 4 °C and then washed in PBS and incubated with Alexa Fluor 488-conjugated secondary antibodies and phalloidin in PBS for 1 h at RT. Coverslips were washed in PBS and mounted with 4,6-diamidino-2-phenylindole (Cat. No. P36931: Thermo Fisher Scientific). The primary antibodies were YAP (1:200) (Cat. No. sc101199: Santa Cruz Biotechnology, Dallas, TX), Ki-67 (1:200) (Cat No. MA5-14520), and HNF4α (1:100) (Cat No. PA5-82159: Thermo Fisher Scientific). The secondary antibodies and dyes (used 1:400) were anti-mouse IgG (H + L) Alexa-488 (Cat. No. A11029: Thermo Fisher Scientific), Alexa Fluor™ 546 Phalloidin (Cat. No. A22283: Thermo Fisher Scientific), and DAPI (Cat No. D9542: Sigma-Aldrich). Images were taken with a Nikon Ti-e Inverted Microscope (Ti Eclipse, C-LHGFI HG Lamp, CFI Plan Fluor 40 × NA 0.6 air objective; Nikon Europe, Amsterdam, Netherlands; Neo sCMOS camera; Andor, Belfast, UK) with NIS elements AR software.

For albumin staining, cells were blocked and permeabilised in 1% w/v bovine serum albumin, 3% donkey serum (Thermo Fisher Scientific) and 0.1% Triton X-100. Primary antibodies for human albumin (Cat. No. A80-129A: Bethyl Laboratories, Montgomery, AL) were applied for 1 h and after wash steps Alexa Fluor-555/647 conjugated secondary antibodies (Cat No. A21432/A21447: Thermo Fisher Scientific) were incubated for 40 min. NucBlue Fixed Cell ReadyProbes Reagent (Thermo Fisher Scientific) was applied for visualization of cell nuclei. Imaging was performed on an Operetta High Content Screening System (PerkinElmer, Waltham, MA).

2.8. Image Quantification

Analysis of immunofluorescence staining was performed as previously described [34]. Briefly, staining intensity was measured in Fiji [35] using the "mean grey value" parameter applied to a region of interest (ROI) created for manually segmented cells based on DIC images. Mean grey values for each image's background were subtracted for each measured staining intensity. Nuclear ROIs were defined through automated thresholding of the DAPI channel in ImageJ. Measurements of the

YAP or HNF4α fluorescence intensity in the nucleus were obtained in ImageJ (measured mean grey value) using the nuclear ROI (co-localisation with DAPI) and for YAP compared against the cytoplasmic YAP staining intensity (measured mean grey value) for the whole image ROI with subtracted nuclear ROIs. Ratios of the nuclear to cytoplasmic fluorescence intensities were calculated. Percentage of HNF4α positive cells were counted as a ratio of DAPI thresholded nuclei expressing at signal at least 50% stronger than the background to total number of nuclei within the ROI.

2.9. Viability and Quantification of dsDNA

To determine cell viability, PrestoBlue Cell Viability Reagent (Thermo Fisher Scientific) was used in accordance with the manufacturer's instructions and normalised against cells on type-1 collagen-coated tissue culture plastic.

To normalise for variance in number, cells were lysed in 350 μl RLT buffer (QIAGEN, Hilden, Germany) and double stranded DNA (dsDNA) was measured using the Quant-iT PicoGreen dsDNA assay kit (Thermo Fisher Scientific). The assay was carried out in accordance with the manufacturer's guidance. If used to quantify cell number, a standard curve using a sample of known cell number was run in parallel to the dsDNA standard curve.

2.10. Enzyme Linked-Immunosorbent Assay (ELISA)

For the assessment of secreted proteins by enzyme linked-immunosorbent assay (ELISA), supernatants were collected from hepatic cell cultures after 48 h of incubation time, and frozen at −20 °C. Albumin production was measured using the Human Albumin Quantification Set (Bethyl Laboratories). Alpha-fetoprotein (AFP) secretion was quantified using the Human Alpha-Fetoprotein ELISA Kit (Alpha Diagnostic International, San Antonio, TX). The presence of Alpha-1-antitrypsin in supernatants was detected using the Human Alpha-1-Antitrypsin ELISA Kit (Abcam, Cambridge, UK). All ELISAs were carried out in accordance with the manufacturer's instructions. Absorbance was measured at 450 nm on a Promega GloMax Multi + Detection System plate reader (Promega, Madison, WI).

2.11. Cytochrome P450 Activity

Native cytochrome P450 activity was assessed using a P450-Glo CYP1A2/2B6/2C9/3A4 Assay Kit (Promega, Madison, MI), in accordance with the manufacturer's instructions. Cells were washed in Ca/Mg^{2+} free PBS before being incubated for 1 h at 37 °C in fully supplemented HepatoZYME-SFM, or PBS containing 3 mM salicylamide, that included the bioluminescent substrate. After incubation, 25 μl of supernatant was transferred into the wells of a white 96-well plate, and mixed with 25 μl of the detection reagent, and incubated for 20 min in the dark at RT. The plate was transferred into a Promega GloMax Discover multimode microplate reader and luminescence measured using a 1 s integration time. The background signal of the assay (no cells) was subtracted from measurements on cell cultures.

2.12. Urea Quantification

Ureagenesis *in vitro* was measured using a QuantiChrom Urea Assay Kit (BioAssay Systems, Hayward, CA). For ammonia challenges, hPSC-Heps were challenged for 48 h in cell culture medium supplemented with 4–5 mM NH_4Cl. Supernatant were collected and immediately analysed for urea content. Absorbance was read at 450 nm on a Promega GloMax Discover multimode microplate reader (Promega, Madison, WI).

2.13. Real-Time PCR

Total RNA was isolated using the RNeasy Mini Kit (QIAGEN, Hilden, Germany) according to manufacturer's protocol. RNA concentration was quantified using a NanoDrop 2000 (Thermo Fisher Scientific, Waltham, MA) and 350 ng of RNA was used to produce cDNA using the SuperScript VILO cDNA synthesis kit (Thermo Fisher Scientific, Waltham, MA). Quantitative real-time PCR (RT-PCR) was performed in a 10 μl reaction mixture consisting of cDNA, custom designed oligonucleotide primers (Sigma–Aldrich, St. Louis, MO) and Fast SYBR Green PCR Master Mix (Thermo Fisher Scientific, Waltham, MA) on a CFX384 Touch Real-Time PCR Detection System (Bio-Rad, Hercules, CA). *GAPDH* and *RPL13A* were used for housekeeping.

2.14. Statistical Analyses

N represents the number of biological replicates of each individual hepatocyte-specific differentiation performed using a stated cell line. Statistical significance ($p < .05$) was determined using Student's T-test (assume Gaussian distribution, two-tailed) or One-way ANOVA followed by Tukey's posthoc test.

3. Results

Emerging evidence suggests that mechanical stiffness which recapitulates native tissue-like environments can impact the differentiation of human liver stem/progenitor cells [22,36] and hPSCs into hepatocytes [37]. To test this explicitly, we created 2D PEG hydrogels with modifiable stiffnesses [26,38] to determine how stiffness impacts hPSC-Heps differentiation independently of ligand density. Our hydrogels are formed through two sequential click reactions. First, PEG-peptide conjugates are formed by reacting an N-terminal amine of a non-functional or RGD sequence-containing peptide with PEG-4NPC. The hydrogel is then formed by a Michael addition between PEG-4VS with a C-terminal free thiol on the peptide (Fig. 1A). Hydrogel *E* is controlled by altering polymer concentration. This design, in which both functional and non-functional peptides participate in cross-linking, allows functional peptide concentration to be held constant as stiffness is altered, or for functional peptide concentration to be varied whilst *E* is held constant (Fig. 1B). We first created "stiff" and "soft" hydrogels with polymer concentrations of either 10% or 2.5%, respectively (Fig. 2A). Atomic force microscopy (AFM) force spectroscopy measurements determined that stiff hydrogels had a median *E* of 19 kPa, similar to that of F2–F3 stage fibrotic human liver [39], and soft hydrogels were just 1.5 kPa, akin to that of the healthy adult liver [40] (Fig. 2B).

Previous studies have been unable to attach hPSC-Heps to type-1 collagen-coated polyacrylamide substrates softer than 20 kPa [41]. Here, hepatic endoderm-stage cells after 14 days of directed differentiation [32] attached to PEG hydrogels in the absence of ROCK inhibitor or FBS and matured as confluent monolayers for 20 days in fully chemically defined, serum-free media (Fig. 2C). We could detect no difference in cell viability (Fig. S1A), and dsDNA quantification revealed no differences in cell number between soft and stiff conditions (Fig. 2D). Moreover, RT-PCR revealed no differences in expression of genes associated with cell cycle progression or proliferation (Fig. S2A), and immunofluorescence staining for Ki-67 could only detect rare, occasional positive nuclei (Fig. S3A). Thus, differences in cell response on soft and stiff hydrogels could not be attributed to cell number or density.

To determine if stiffness impacted hPSC-Hep function, we first assayed cells' albumin production rate and found that it was significantly higher for cells on soft hydrogels compared to stiff (Fig. 2E). The metabolic activity of hepatocytes is central to their function and largely depends on the activity of enzymes in the cytochrome P450 family. We measured cytochrome 1A2, 2B6, 2C9 and 3A4 activity, and found that all were increased in hPSC-Heps cultured on soft hydrogels compared to stiff (Fig. 2F). One important role of healthy hepatocytes is to detoxify

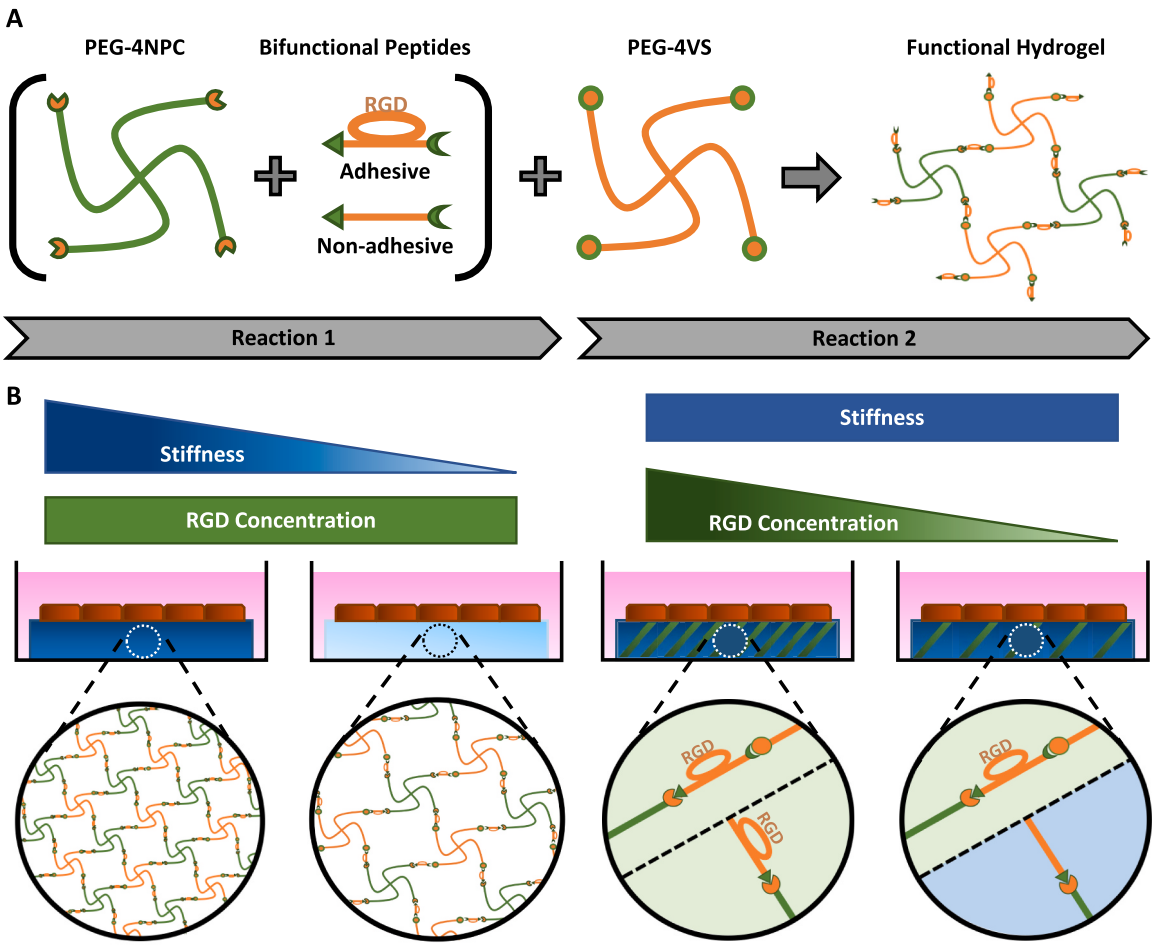

Fig. 1. Designing modular biomimetic PEG-peptide hydrogels for optimised hepatocyte differentiation. **(A)** Schematic figure showing the two reaction steps to fabricate hydrogels. The first reaction conjugates peptides with PEG-4NPC. The second reaction selectively cross-links PEG-peptide conjugates with PEG-4VS using a Michael-type addition. **(B)** Illustrative figure highlighting our biomaterials' independent control of polymer concentration/stiffness vs concentration of RGD-motif-containing peptides.

ammonia. Thus, urea synthesis is often used to monitor their functionality. When hPSC-Heps matured on soft hydrogels were treated for 48 h with 4 mM NH_4Cl, we measured a significant increase in urea within the culture media supernatant compared to cultures on stiff hydrogels (Fig. 2G).

To further validate our hepatic phenotype, we performed RT-PCR on a panel of hepatocyte markers including *ALB* and *AHSG* that encode key serum proteins; *ASGR2,* which plays a crucial role in serum glycoprotein homeostasis; cytochrome P450 genes *CYP2E1* (ethanol oxidation), *CYP3A4* (xenobiotic metabolism), and *CYP7A1* (cholesterol homeostasis); *FABP1,* which is known to be critical for fatty acid uptake and intracellular transport; and SERPINF2, which encodes alpha 2-antiplasmin and regulates the blood clotting pathway. Expression of all of these genes was elevated in hPSC-Heps cultured on soft hydrogels when compared to stiff (Fig. 3A). Additionally, a moderate but significant reduction in expression was measured for *KRT19* (embryonal hepatocyte cytokeratin). No difference in expression was measured for *SERPINA1* or the protein that it encodes, alpha-1-antitrypsin (Fig. S1B). Furthermore, RT-PCR revealed significant upregulation of genes associated with liver fibrosis in hPSC-Heps cultured on stiff hydrogels (Fig. S2B).

As *HNF4A* is a central regulator of hepatocyte differentiation and in murine hepatocytes has been shown to respond to matrix rigidity [21], we initially hypothesised that improvements in hepatic function might be attributable to increased *HNF4A* expression. However, we could detect no difference in *HNF4A* expression between conditions (Fig. 3B), suggesting that the improved albumin production, cytochrome p450 activity, and urea synthesis occurred independently of increased *HNF4A* expression. Moreover, immunofluorescence staining for HNF4α revealed that there was no difference in the number of positive nuclei or mean fluorescence intensity (Fig. S3B). We could also detect no difference in expression levels of *HNF1B*, whose promoter is bound by HNF4α during liver development, driving its transcription [42]. Contrastingly, we could detect significant increases in the expression of liver-enriched transcription factors, *CEBPA* and *HNF6,* within hPSC-Heps matured on soft hydrogels. Furthermore, the expression of the transcriptional coactivator *PPARGC1A* was also increased on soft PEG substrates (Fig. 3B).

Active YAP within mouse hepatocytes has been shown to suppress PGC1α – encoded (in human cells) by *PPARGC1A* [43], and YAP/TAZ depletion was found to increase *Cebpa* expression [44]. Therefore, we hypothesised that the improved hepatocyte maturation on soft substrates could be due to decreased expression of YAP/TAZ. RT-PCR revealed that expression of *YAP1* (YAP), *WWTR1* (TAZ), and their target genes *CTGF* and *CYR61* were all significantly lower in hPSC-Heps matured on soft compared to stiff hydrogels (Fig. 3C) (although we could detect no difference in expression of *ANKRD1*). TGFβ expression in hepatocytes is a hallmark of fibrotic liver diseases [45,46], and active YAP results in TGFβ-dependent epithelial-to-mesenchymal transition of hepatocytes [47]. In agreement with reduced *YAP1* expression, we also observed significantly reduced expression of *TGFB*, *TGFBR1*, *SMAD2*, and *SMAD3* in hPSC-Heps on soft hydrogels (Fig. S4A). Moreover,

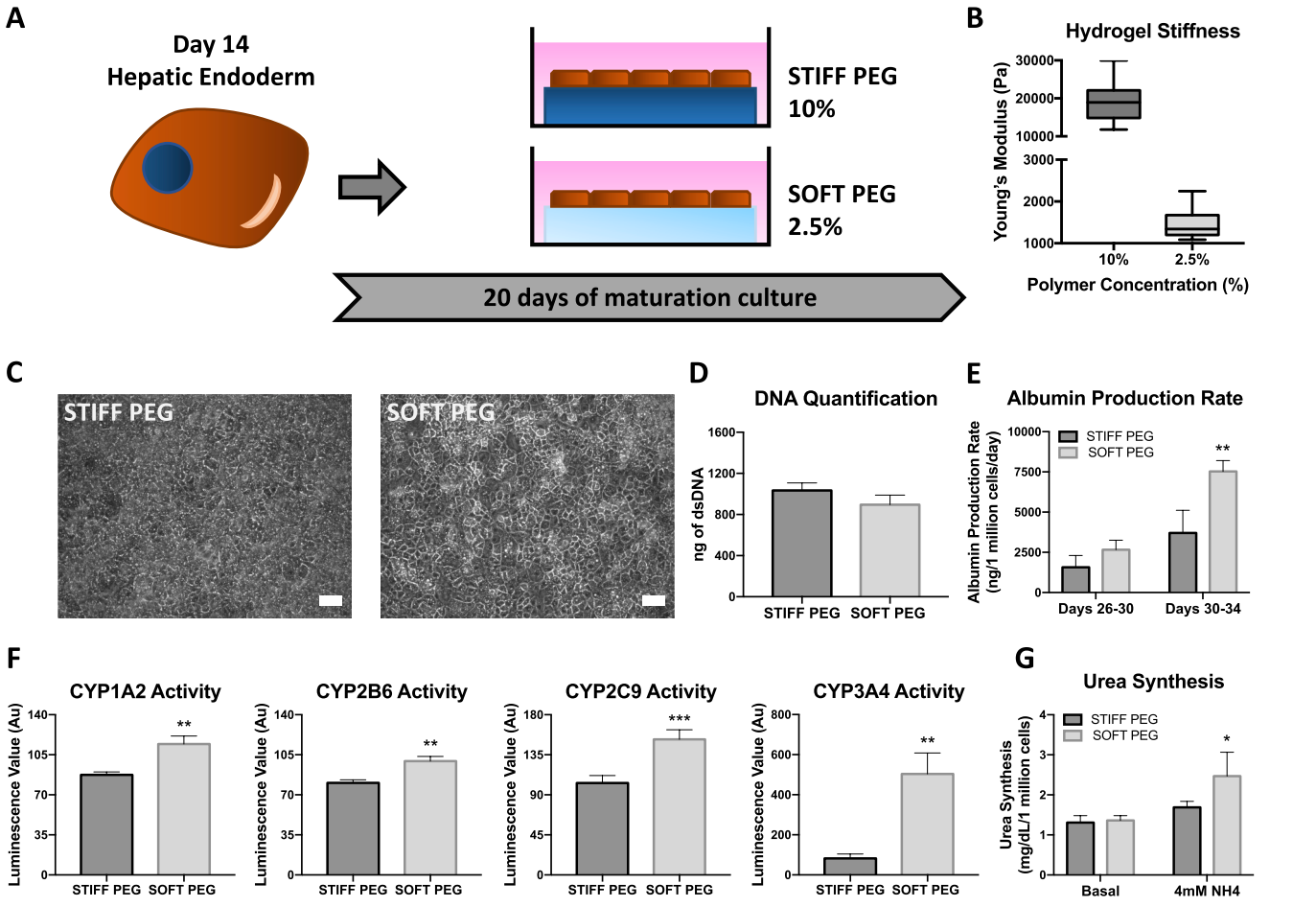

Fig. 2. Mimicking healthy liver physiological stiffness improves hepatocyte differentiation in 2D. **(A)** Experimental design schematic; day 14 hPSC-derived hepatic endoderm-stage cells are seeded onto modular biomimetic hydrogels of 10% (STIFF PEG) or 2.5% (SOFT PEG) polymer concentration for 20 days of maturation culture. **(B)** Atomic force microscopy measurements of the Young's Modulus of hydrogel formulations. **(C)** Brightfield microscopy images of confluent hPSC-Heps 3 days after seeding onto PEG hydrogels of different stiffness; cell line 1. **(D)** Quantification of double stranded DNA (dsDNA) collected from 2D PEG substrate cultures after 20 days of culture, n = 5 experiments. Data are mean ± SD. Data shown for cell line 2. **(E)** Albumin production rate of hPSC-Heps cultured on 2D PEG hydrogels (Dark grey bars: STIFF PEG; Light grey bars: SOFT PEG), n = 5 experiments. Data are mean ± SD, **, $p < .01$. Data shown for cell line 1. **(F)** Cytochrome P450 1A2, 2B6, 2C9 and 3A4 enzyme activity of hPSC-Heps cultured on 2D PEG hydrogels, n = 5 experiments. Data are mean ± SD, **, $p < .01$. Data shown for cell line 2. **(G)** Urea synthesis by hPSC-Heps cultured on 2D PEG hydrogels, n = 5 experiments. Data are mean ± SD, *, $p < .05$. Data shown for cell line 3. Scale bars, 100 μm.

RT-PCR revealed evidence of supressed HGF signalling in hPSC-Heps on soft hydrogels (Fig. S4B). When we targeted this pathway to enhance the differentiation of hPSC-Heps on type-1 collagen-coated tissue culture plastic (TCP) (Fig. S4C), we found that whilst the removal of HGF did not change albumin expression or urea synthesis, it did significantly enhance the activity of cytochrome p450 (Figs. S4D–F).

When YAP signalling is active, the protein is located in the nucleus. To confirm our mRNA observations, we performed immunofluorescence staining. Quantification of the nuclear/cytoplasmic signal ratio revealed significantly less nuclear YAP in cells on soft hydrogels (Fig. 4A). As YAP activity inversely correlated with hPSC-Hep functionality, we next sought to determine if reducing integrin-mediated YAP activity during hepatocyte differentiation on type-1 collagen-coated glass could prompt hPSC-Heps to adopt improved metabolic functionality.

As *ITGB1* is part of the largest integrin family [48] and as fetal hepatocytes express *ITGB1*, which later decreases as human liver organogenesis proceeds [49], we elected to transfect hepatic endoderm-stage cells with siRNA to knockdown *ITGB1* (Fig. 4B). RT-PCR confirmed that *ITGB1* had been efficiently knocked down (Fig. 4C), and that whilst there was no significant reduction in *YAP1*, there was significant reduction in the expression of YAP target genes *CTGF* and *CYR61*, and a modest reduction to *ANKRD1* (Fig. 4D). Despite the early timepoint in the differentiation protocol, we also observed an increase in *ALB* expression, and increases to *CYP2E1* and *CYP3A7*. Furthermore, we found significant increases in expression levels of *CYP7A1* and *CPS1*, which encodes the protein that catalyses the first and rate-limiting step of the urea cycle (Fig. 4E).

As the addition of small molecules may be more amenable to larger scale manufacturing of hPSC-Heps than siRNA transfection, we next explored whether improved metabolic functionality could be achieved with small molecule inhibitors of YAP/TAZ signalling such as Forskolin (FSK) and Verteporfin (VP) (Fig. S5A). RT-PCR confirmed that FSK or VP treatment resulted in a decrease in YAP target gene (*CTGF*) expression, but no impediment to hepatocyte differentiation (*ALB* & *CYP7A1*) (Fig. S5B). Interestingly, we also observed a decrease in *ITGB1* expression after VP treatment. Immunofluorescence staining for albumin revealed a significant increase in expression in hPSC-Heps treated with VP [50] (Fig. S5C). We also evaluated changes to hepatic metabolic function by assaying the activity of cytochrome p450 enzymes. Treatment with FSK did not alter 1A2 activity, but did result in significant increases in 2B6 and 3A4 activity. Similarly, treatment with VP resulted in significantly greater activity of all three enzymes (Fig. S5D).

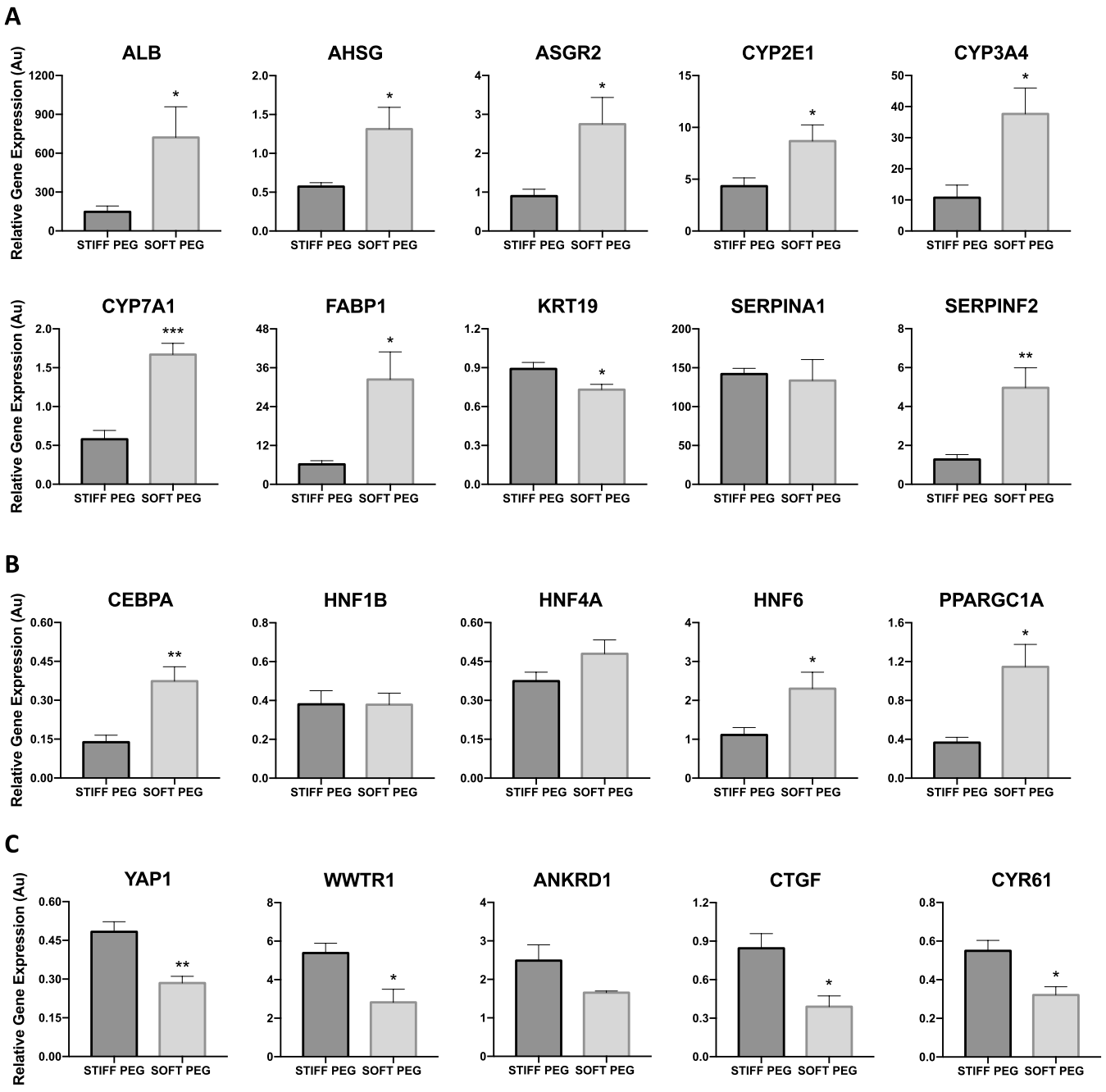

Fig. 3. Substrate stiffness influences hepatic and YAP/TAZ gene expression. Differential gene expression showing the relative expression of mRNA associated with **(A)** hepatocyte functionality **(B)** transcriptional regulation, and **(C)** YAP/TAZ activity within hPSC-Heps after 20 days of maturation culture, n = 5 experiments. Data are mean ± SD, *, p < .05; **, *p* < .01; ***, p < .001. Data shown for cell line 2.

Targeting the actin cytoskeleton of murine hepatocytes reduces mechanical tension-induced YAP activity and maintains metabolic functions [51]. When we treated hPSC-Heps with Y-27632 dihydrochloride (actomyosin contraction) or Latrunculin A (actin polymerisation), we observed evidence of poor hepatocyte differentiation and impaired metabolic (including cytochrome p450) function (Figs. S6A and B). Moreover, when we challenged cultures with 5 mM NH_4Cl we found that FSK treatment resulted in a significant increase in the amount of urea detected in the culture supernatant (Fig. S5E). Intriguingly, treatment with VP did not enhance ureagenesis, as we could detect no differences in treated cells compared to controls, suggesting that YAP-mediated suppression of ureagenesis is independent from YAP-TEAD interactions. This was further supported by siRNA knockdown of *YAP1*, *TEAD1*, or *TEAD4*. Knockdown of either TEAD did not result in measurable changes in *CPS1* expression, whereas the mean expression was ~750× higher after *YAP1* knockdown (Figs. S7A and B). Together, these data reveal that active YAP impairs the differentiation and key metabolic functions of hPSC-Heps.

As our data suggested mechanosensing-mediated cellular responses, we next hypothesised that stiffness was driving hepatocyte functionality by altering expression of genes involved in cell-ECM and/or cell-cell interactions. Whilst we found no evidence of regulation of genes encoding components of Notch-signalling - a highly conserved cell–cell communication pathway (Fig. S2C), the expression of RGD-binding integrins *ITGB1* and *ITGB3*, but not *ITGB5*, were lower on soft hydrogels compared to stiff (Fig. 5A). Therefore, we next fabricated hydrogels

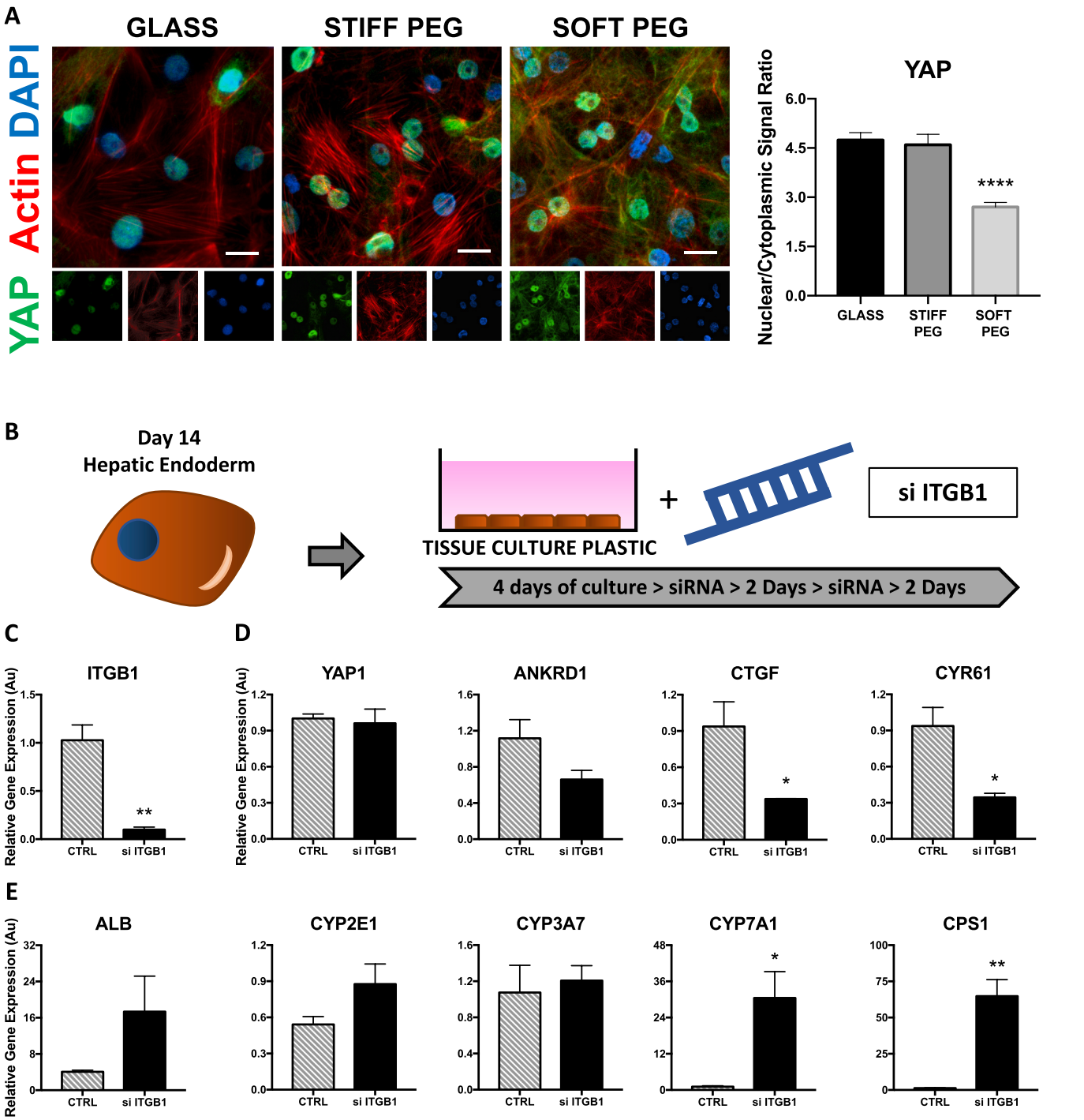

Fig. 4. Targeting YAP activity with siRNA to improve hepatocyte differentiation. **(A)** YAP immunofluorescence staining (left) and nuclear/cytoplasmic signal ratio (right) of hPSC-Heps cultured for 72 h on type-1 collagen-coated glass or 2D hydrogels of 10% (STIFF PEG) or 2.5% (SOFT PEG) polymer concentration containing 1770 μM RGD motif peptides, n = 3 experiments. Data are mean ± SD, ****, p < .0001. Data shown for cell line 1. Scale bars, 100 μm. **(B)** Experimental design schematic; day 14 hPSC-derived hepatic endoderm-stage cells are seeded into maturation culture on type-1 collagen-coated tissue culture plastic and after 4 days were transfected with scrambled siRNA (CTRL) or siRNA targeting *ITGB1* (si ITGB1). Following a further 48 h the cells were transfected again and cultured for 2 days. **(C)** Differential gene expression showing the relative expression of *ITGB1* **(D)** *YAP1* and target genes and **(E)** mRNA associated with hepatocyte functionality, n = 3 experiments. Data are mean ± SD, *, p < .05; **, *p* < .01. Data shown for cell line 1.

with altered concentrations of RGD motif-containing peptides. Hydrogels containing non-adhesive peptide sequences (no RGD motif) alone did not allow for cell attachment (Fig. 5B). However, hPSC-Heps formed confluent monolayers on stiff hydrogels that either maintained the RGD concentration in our previous experiments (1770 μM, HIGH RGD) or had a reduced RGD concentration (885 μM, LOW RGD) (Fig. 5C). Reduced RGD concentration did not prevent cell attachment, nor the formation of confluent monolayers (Fig. 5D). dsDNA quantification also revealed no differences in cell number between conditions (Fig. 5E); however, we found that on stiff hydrogels, reduced RGD concentration prompted elevated albumin production rates (Fig. 5F) and increased cytochrome p450 activity (Fig. 5G). Furthermore, hPSC-Heps on LOW RGD

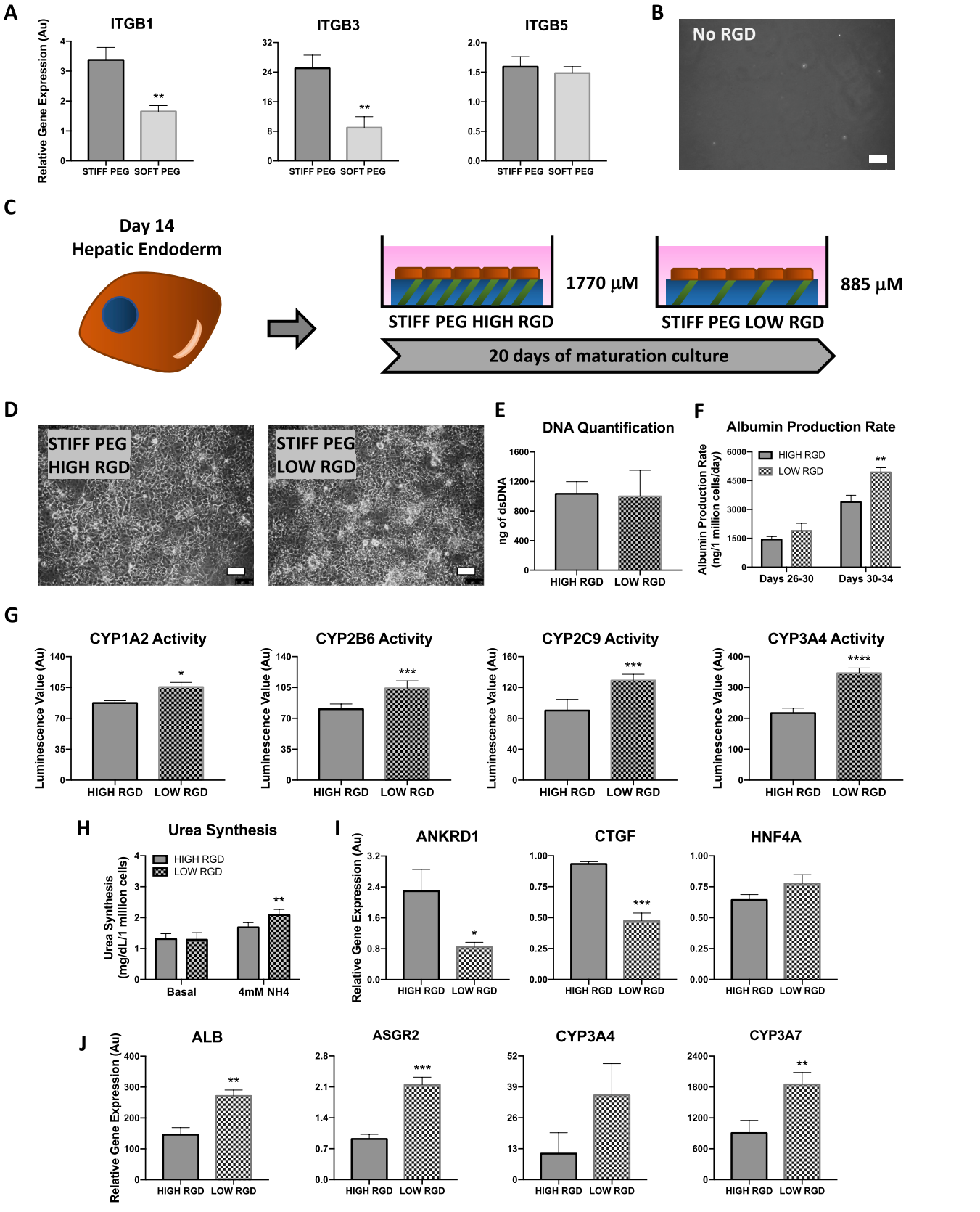

(caption on next page)

Fig. 5. The role of RGD peptide concentration in hepatocyte differentiation on STIFF PEG. **(A)** Differential gene expression showing the relative expression of mRNA associated with RGD-mediated integrin binding correlates with increased substrate stiffness, n = 5 experiments. Data are mean ± SD, **, $p < .01$. Data shown for cell line 2. **(B)** Brightfield microscopy image showing that without the inclusion of peptides that contain the RGD-motif, hPSC-derived endoderm-stage cells cannot adhere to the hydrogel. **(C)** Experimental design schematic; day 14 hPSC-derived hepatic endoderm-stage cells are seeded onto 10% polymer concentration (STIFF PEG) modular biomimetic hydrogels, containing either 1770 μM (HIGH RGD) or 885 μM (LOW RGD) RGD-motif-containing peptides, for 20 days of maturation culture. **(D)** Brightfield microscopy images of confluent hPSC-Heps 3 days after seeding onto PEG hydrogels with different RGD-motif-containing peptide concentrations; cell line 1. **(E)** Quantification of double stranded DNA (dsDNA) collected from 2D PEG substrate cultures after 20 days of culture, n = 5 experiments. Data are mean ± SD. Data shown for cell line 1. **(F)** Albumin production rate of hPSC-Heps cultured on 2D PEG hydrogels (Dark grey bars: HIGH RGD STIFF PEG; Chequered bars: LOW RGD STIFF PEG), n = 5 experiments. Data are mean ± SD, **, $p < .01$. Data shown for cell line 1. **(G)** Cytochrome P450 1A2, 2B6, 2C9 and 3A4 enzyme activity of hPSC-Heps cultured on 2D PEG hydrogels, n = 5 experiments. Data are mean ± SD, *, $p < .05$; ***, $p < .001$; ****, $p < .0001$. Data shown for cell line 1. **(H)** Urea synthesis by hPSC-Heps cultured on 2D STIFF PEG hydrogels, n = 5 experiments. Data are mean ± SD, **, $p < .01$. Data shown for cell line 3. Differential gene expression showing the relative expression of mRNA associated with **(I)** YAP/TAZ activity and **(J)** hepatocyte functionality within hPSC-Heps after 20 days of maturation culture, n = 5 experiments. Data are mean ± SD, *, $p < .05$; **, $p < .01$; ***, $p < .001$. Data shown for cell line 1. Scale bars, 100 μm.

hydrogels produced more urea than those on HIGH RGD hydrogels when cultured in the presence of 4 mM NH_4Cl (Fig. 5H). We also found decreased expression of YAP/TAZ target genes on LOW RGD gels and significantly reduced nuclear localisation of YAP protein (Fig. S8), which correlated with improved hepatocyte function. Moreover, changes in hepatic function were independent of changes in *HNF4A* expression (Fig. 5I). To further confirm improved hepatocyte differentiation, we conducted RT-PCR and found increased expression of *ALB, ASGR2* and *CYP3A7* in hPSC-Heps on the LOW RGD compared to HIGH RGD (Fig. 5J). Taken together, these data suggest that biomaterial stiffness and ligand density converge on the Hippo pathway to influence the differentiation of hPSC-Heps.

As reducing RGD concentration improved hPSC-Hep differentiation and function on stiff hydrogels, we next asked if further improvements on soft hydrogels could be achieved by reducing the concentration of RGD-containing peptides (Fig. 6A). Reducing RGD concentration on soft hydrogels did not prevent cellular attachment, nor the formation of confluent monolayers (Fig. 6B), and did not impact cell numbers (Fig. 6C). However, we found that hPSC-Hep secretion of albumin, cytochrome P450 activity and urea synthesis were all lower when cultured on soft hydrogels in the LOW RGD condition compared to the HIGH (Fig. 6D–F). Moreover, on soft hydrogels, LOW RGD prompted significantly higher expression of YAP/TAZ target genes, and despite reduced hepatic functionality, increased *HNF4A* expression (Fig. 6G). Unexpectedly, no change was observed in the YAP nuclear-to-cytoplastic ratio (Fig. S8). This compromised hepatocyte differentiation was further confirmed by RT-PCR, which revealed significantly reduced expression levels for *ALB*, *ASGR2*, *CYP3A4* and *CYP3A7* (Fig. 6H). Taken together, these data show that when differentiated on either soft or stiff substrates, adhesive ligand concentration-induced reduction in YAP/TAZ activity was correlated with increases in key markers of hepatocyte metabolic function.

Having established that functionality of hPSC-Heps could be enhanced through controlling biomaterial stiffness or RGD ligand concentration, we next sought to benchmark our hPSC-Heps against cells produced using chemical differentiation protocols on TCP coated with type-1 collagen (Fig. 7A). After 20 days of differentiation, confluent monolayers were evident on both TCP and soft PEG conditions (HIGH RGD, Fig. 7B). However, culture on soft gels resulted in significantly greater albumin production, alpha-1-antitrypsin production, cytochrome P450 activity and urea synthesis when compared to TCP (Fig. 7C–F). We also observed that expression of YAP/TAZ target genes was significantly lower in hPSC-Heps on the soft gels, and that the expression of *HNF4A* was significantly elevated compared to that in cells cultured on TCP (Fig. 7G). hPSC-Heps also showed improved differentiation on soft hydrogels compared to TCP, as we observed significantly increased expression of a range of hepatocyte genes (Fig. 7H).

Delivery of hPSC-Heps for cellular therapy may require encapsulation within a biomaterial. Having established that hepatocyte metabolic functionality could be influenced by PEG hydrogel stiffness in 2D, we next sought to determine if the same was true for 3D encapsulated cells. To test this, we encapsulated day 14 hepatic endoderm-stage cells within soft and stiff hydrogels (HIGH RGD) and confirmed that cell viability was no different between conditions (Fig. S9A). Like 2D cultures, we found that albumin production rates were higher for hPSC-Heps cultured within the soft compared to stiff hydrogels (Fig. S9B). As altering RGD concentration influenced hPSC-Hep in 2D, we next encapsulated cells within soft and stiff hydrogels with either HIGH RGD or LOW RGD concentrations (Fig. 8A; Fig. S9C). There was no difference in viability (Fig. 8B); however, reducing RGD-motif peptide concentration in soft hydrogels resulted in significantly lower albumin protein production (Fig. 8C), decreased cytochrome P450 3A4 enzyme activity (Fig. 8D), and inferior urea synthesis after being challenged with 5 mM NH_4Cl (Fig. 8E). Interestingly, whilst minor improvements were seen when RGD concentration was reduced in stiff hydrogels, differences were not significant for any of the three assays.

We next asked if 3D encapsulation could enhance hepatocyte differentiation compared to 2D culture on hydrogels. As in both 2D and 3D cultures, hPSC-Hep metabolic functionality appeared to be superior in soft conditions with HIGH RGD, this hydrogel formulation was used for both 2D and 3D conditions. After 8 days of culture, we found no difference in the expression of hepatocyte differentiation markers *AFP*, *ALB* or *HNF4A* when comparing soft 2D to 3D conditions (Fig. S9D). Similarly, at this early (immature hepatocyte) timepoint there was no difference in alpha-fetoprotein production (Fig. S9E). Whilst albumin production rates were no different after 20 days of culture (Fig. 8F), we did measure a significant reduction in secreted alpha-fetoprotein in hPSC-Heps cultured in 3D hydrogels (Fig. 8G), and downregulation (although not significant) of *AFP* expression. We identified no difference in *ALB* or *HNF4A* expression (Fig. 8H). Alpha-fetoprotein is a fetal serum protein that is absent in normal adult serum. Although many markers of hepatocyte function remained unchanged, this reduction in alpha-fetoprotein production suggests that 3D culture results in a hPSC-Hep phenotype more closely resembling bona fide hepatocytes.

We [32,52] and others [53–55] have proposed alginate microencapsulation of hepatocytes as an approach to treat acute liver failure. However, for islet transplantation, PEG-based materials have shown advantages over alginate as they supported superior long-term cell function upon transplantation into ectopic sites [56]. We encapsulated hPSC-Heps into either soft PEG (HIGH RGD) or alginate hydrogels (1.8% ultra-pure low viscosity, high glucuronic acid) (Fig. 8I). We found that hPSC-Heps within soft PEG hydrogels produced significantly higher levels of albumin and metabolised more urea (Fig. 8J and K). These data suggest that future studies using biomaterials to deliver hepatocytes should investigate the potential of PEG-based hydrogels.

4. Discussion

Cells receive both mechanical and biological cues from their environment, which impacts their function [57]. However, few studies have explored the impact of native tissue-like stiffnesses on the differentiation of hPSCs into hepatocytes. hPSC-Heps cultured on type-1 collagen--coated polyacrylamide produced more albumin as substrate *E* was decreased from 140 to 20 kPa [41]. However, as the healthy human

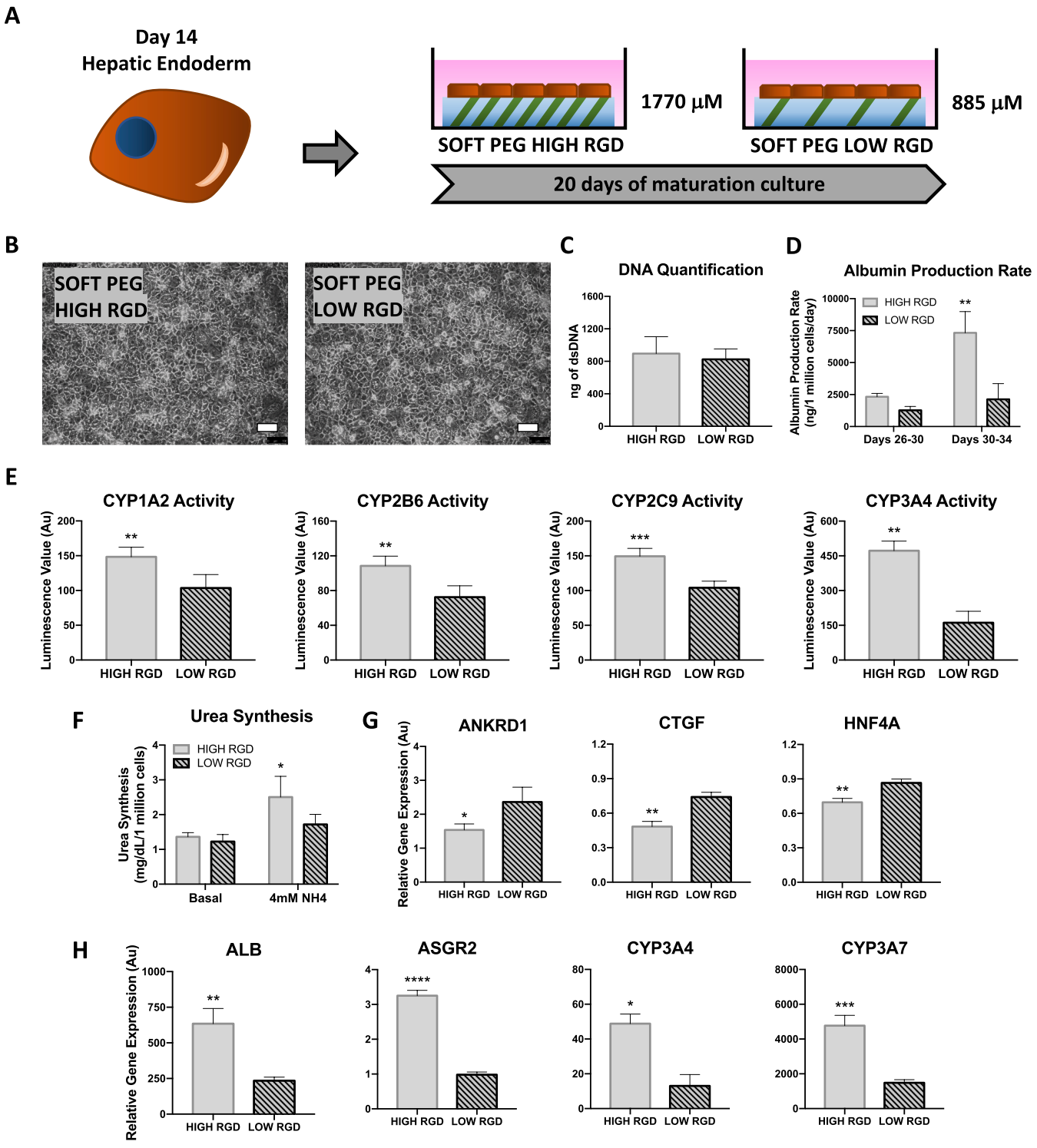

Fig. 6. The role of RGD peptide concentration in hepatocyte differentiation on SOFT PEG. **(A)** Experimental design schematic; day 14 hPSC-derived hepatic endoderm-stage cells are seeded onto 2.5% polymer concentration (SOFT PEG) modular biomimetic hydrogels, containing either 1770 µM (HIGH RGD) or 885 µM (LOW RGD) RGD-motif-containing peptides, for 20 days of maturation culture. **(B)** Brightfield microscopy images of confluent hPSC-Heps 3 days after seeding onto PEG hydrogels with different RGD-motif-containing peptide concentrations; cell line 1. **(C)** Quantification of double stranded DNA (dsDNA) collected from 2D PEG substrate cultures after 20 days of culture, n = 5 experiments. Data are mean ± SD. Data shown for cell line 1. **(D)** Albumin production rate of hPSC-Heps cultured on 2D PEG hydrogels (Light grey bars: HIGH RGD SOFT PEG; Dark striped bars: LOW RGD SOFT PEG), n = 5 experiments. Data are mean ± SD, **, $p < .01$. Data shown for cell line 1. **(E)** Cytochrome P450 1A2, 2B6, 2C9 and 3A4 enzyme activity of hPSC-Heps cultured on 2D PEG hydrogels, n = 5 experiments. Data are mean ± SD, **, $p < .01$; ***, $p < .001$. Data shown for cell line 1. **(F)** Urea synthesis by hPSC-Heps cultured on 2D SOFT PEG hydrogels, n = 5 experiments. Data are mean ± SD, *, $p < .05$. Data shown for cell line 3. Differential gene expression showing the relative expression of mRNA associated with **(G)** YAP/TAZ activity and **(H)** hepatocyte functionality within hPSC-Heps after 20 days of maturation culture, n = 5 experiments. Data are mean ± SD, *, $p < .05$; **, $p < .01$; ***, $p < .001$; ****, $p<.0001$. Data shown for cell line 1. Scale bars, 100 µm.

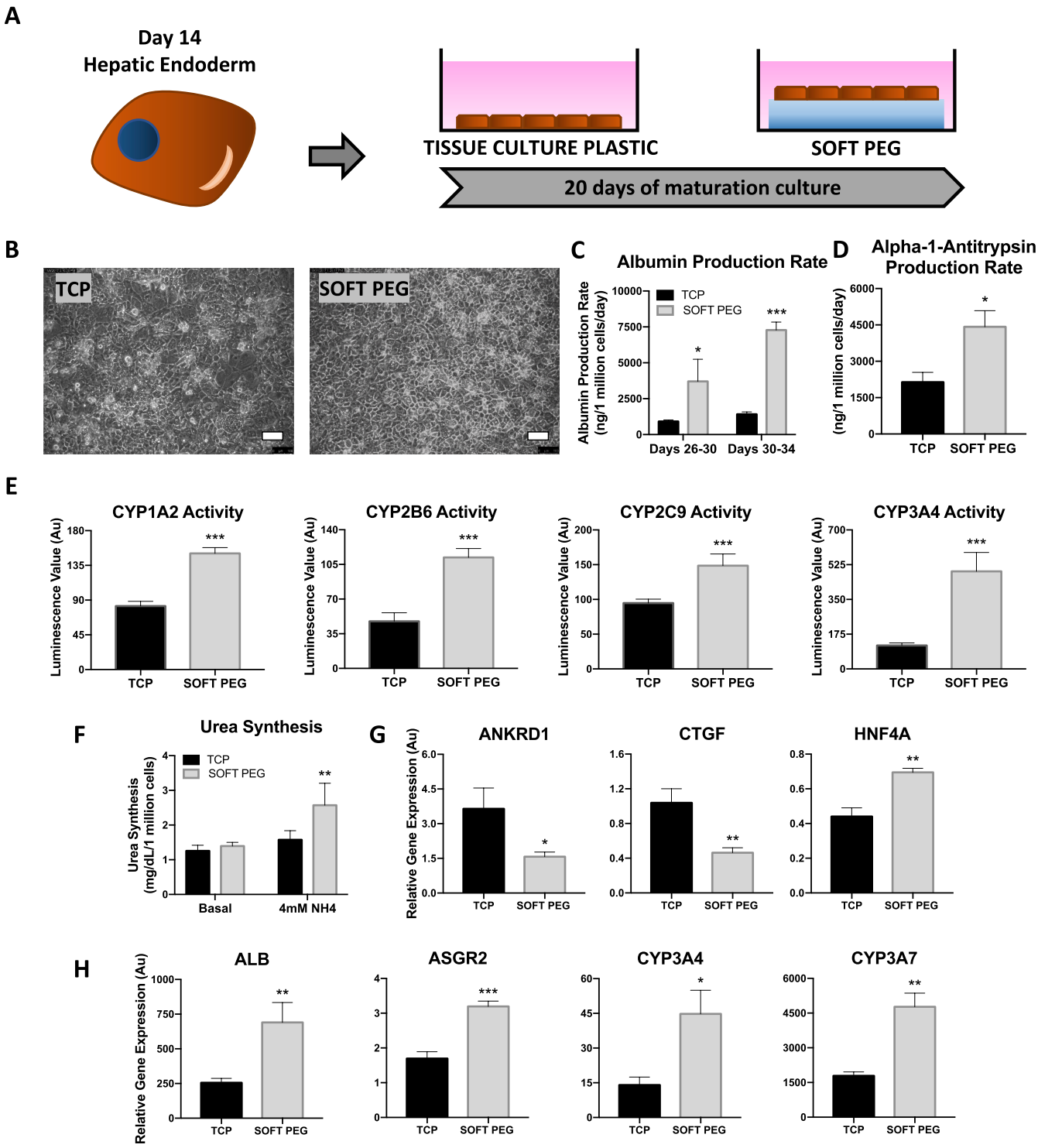

Fig. 7. Hepatocyte differentiation is enhanced on physiologically soft hydrogels compared to conventional tissue culture plastic. **(A)** Experimental design schematic; day 14 hPSC-derived hepatic endoderm-stage cells are seeded onto type-1 collagen-coated tissue culture plastic or 2.5% polymer concentration (SOFT PEG) hydrogels (containing 1770 μM RGD-motif-containing peptide), for 20 days of maturation culture. **(B)** Brightfield microscopy images of confluent hPSC-Heps 3 days after seeding onto type-1 collagen-coated tissue culture plastic or 2.5% polymer concentration (SOFT PEG) modular biomimetic hydrogels; cell line 1. **(C)** Albumin production rate of hPSC-Heps cultured on type-1 collagen-coated tissue culture plastic (TCP) or SOFT PEG hydrogels (Black bars: TCP; Light grey bars: HIGH RGD SOFT PEG), n = 5 experiments. Data are mean ± SD, **, $p < .01$. Data shown for cell line 3. **(D)** Alpha-1-Antitrypsin production of rate of hPSC-Heps cultured on type-1 collagen-coated tissue culture plastic (TCP) or SOFT PEG hydrogels, n = 5 experiments. Data are mean ± SD, *, $p < .05$. Data shown for cell line 3. **(E)** Cytochrome P450 1A2, 2B6, 2C9 and 3A4 enzyme activity of hPSC-Heps cultured on type-1 collagen-coated TCP or SOFT PEG hydrogels, n = 5 experiments. Data are mean ± SD, ***, p < .001. Data shown for cell line 1. **(F)** Urea synthesis by hPSC-Heps cultured on type-1 collagen-coated tissue culture plastic (TCP) or SOFT PEG hydrogels, n = 5 experiments. Data are mean ± SD, **, $p < .01$. Data shown for cell line 3. Differential gene expression showing the relative expression of mRNA associated with **(G)** YAP/TAZ activity and **(H)** hepatocyte functionality within hPSC-Heps after 20 days of maturation culture, n = 5 experiments. Data are mean ± SD, *, p < .05; **, p < .01; ***, p < .001. Data shown for cell line 1. Scale bars, 100 μm.

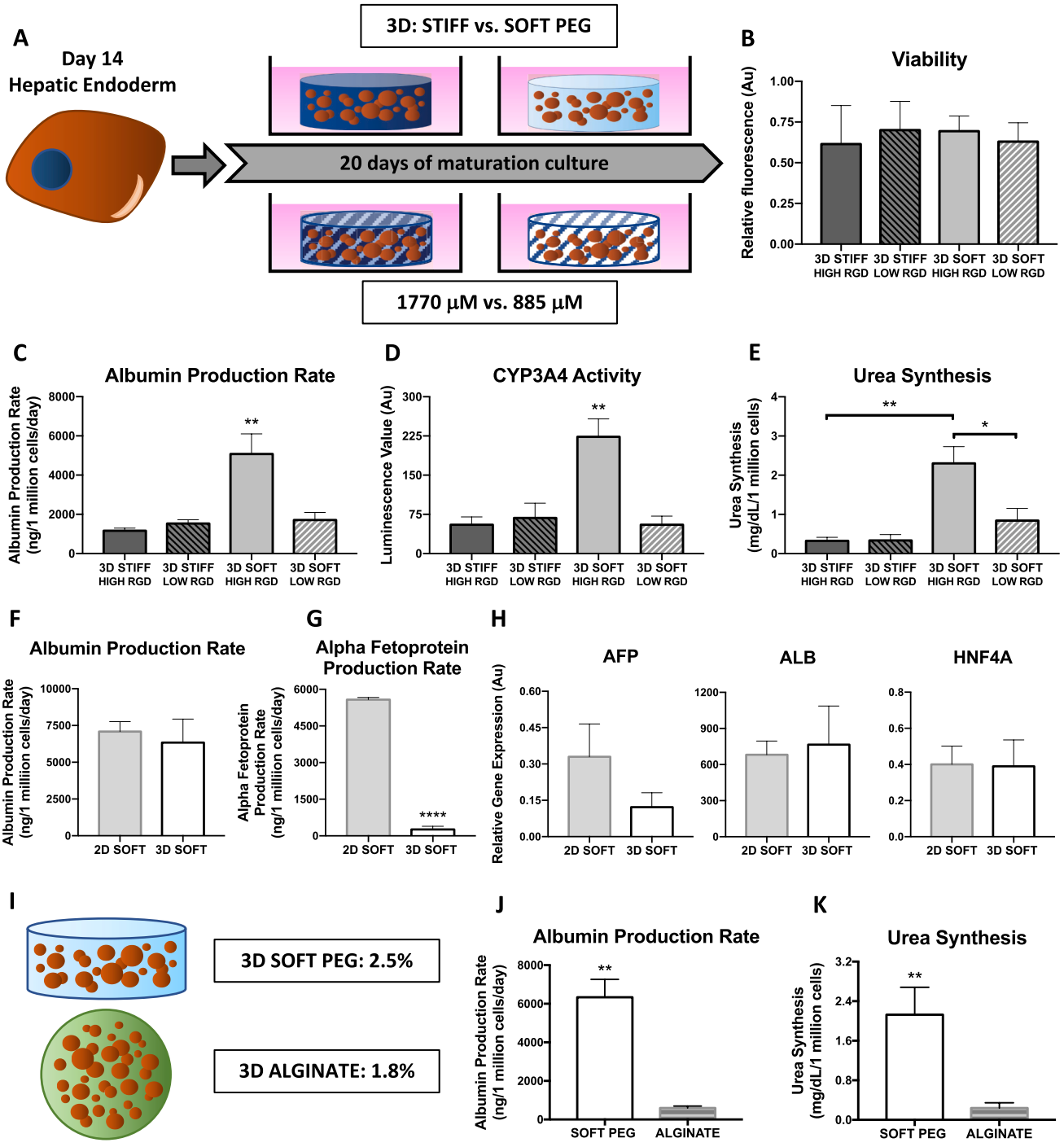

Fig. 8. Modelling the hepatic niche in 3D. **(A)** Experimental design schematic; day 14 hPSC-derived hepatic endoderm-stage cells are encapsulated into hydrogels with 10% (3D STIFF PEG) or 2.5% (3D SOFT PEG) polymer concentrations, each containing either 1770 μM (HIGH RGD) or 885 μM (LOW RGD) RGD-motif-containing peptides. **(B)** Cell viability 24 h after encapsulation within 3D STIFF (Dark grey) or 3D SOFT (Light grey) PEG hydrogels; solid coloured bars = HIGH RGD; striped bars = LOW RGD, n = 4 experiments. Data shown for Cell line 3. **(C)** Albumin production rate, **(D)** CYP3A4 activity and **(E)** Urea synthesis of hPSC-Heps differentiated for 20 days within modular 3D hydrogels of different stiffness and RGD-motif-containing peptide concentration, n = 4 experiments. Data are mean ± SD, *, $p < .05$; **, $p < .01$. Urea synthesis measured in the presence of 5 mM NH_4CL culture media supplementation. Data shown for cell line 3. **(F)** Albumin production rate and **(G)** Alpha-fetoprotein production rate of hPSC-Heps cultured for 20 days on 2D SOFT PEG or within 3D SOFT PEG hydrogels, n = 3 experiments. Data are mean ± SD, ****, $p < .0001$. Data shown for cell line 4. **(H)** Differential gene expression showing the relative expression of mRNA associated with hepatocyte function (*AFP* and *ALB*) and transcription (*HNF4A*) after 20 days of culture, n = 3 experiments. Data are mean ± SD. Data shown for cell line 4. **(I)** Experimental design schematic; single cell suspensions of hPSC-Heps encapsulated into either 3D SOFT PEG (HIGH RGD) or alginate hydrogels (1.8% ultra-pure low viscosity, high glucuronic acid). **(J)** Albumin production rate and **(K)** Urea synthesis of encapsulated hPSC-Heps, n = 5 experiments. Data are mean ± SD, **, $p < .01$. Data shown for cell line 3.

adult liver is considerably softer than 20 kPa, this finding opens the possibility that biomaterials with stiffnesses akin to the native organ may better promote a functional hepatocyte phenotype. We developed PEG-based hydrogels that allow precise control over mechanical properties independently of ligand density, and thus are ideal for exploring the role of cellular mechanosensing in hPSC-Hep differentiation.

While chemically defined differentiation protocols have reported that hPSC can be directed to adopt adult hepatocyte-like functions [32,58,59], here we found that differentiation could be further improved when the *E* of the underlying substrate matched that of the native tissue. It is known that cultured hepatic cells have reduced cytochrome P450 activities in comparison to the human liver [60], but the mechanism(s) responsible for this disparity remains elusive. Here, we detected a pronounced increase in basal cytochrome p450 activity, particularly for the 3A4 isoform, which plays important roles in the detoxification of bile acids, metabolism of steroid hormones, and elimination of phytochemicals present in foods and medications [61,62].

Having identified a role for substrate stiffness in hPSC-Hep differentiation, we probed deeper into the mechanisms driving this response and found reduced expression of YAP/TAZ and their target genes. Integrin-mediated activation of YAP has been implicated in liver fibrosis [63]. Accordingly, knockdown of *ITGB1* within hPSC-Heps by siRNA transfection resulted in decreased YAP target gene expression and a marked increase in expression of genes associated with metabolic function – in particular both *CYP7A1*, which is vital for cholesterol metabolism as it encodes the first and rate limiting enzyme in bile acid synthesis, and *CPS1*. Importantly in liver cells, *CPS1* transcription correlates with protein expression and the ability to perform ammonia detoxification [64], which is considered a key function for cell therapy applications of hPSC-Heps [32].

Verteporfin can inhibit YAP-TEAD interactions and suppresses YAP-induced hepatomegaly in an inducible YAP transgenic mouse model [50], and forskolin has been shown to increase the phosphorylation and cytoplasmic retention of YAP [65,66]. When differentiated in the presence of verteporfin, we found that hPSC-Heps had increased cytochrome p450 enzymes activity. Moreover, upon treatment with forskolin, we observed a dramatic increase in urea synthesis, along with increases in cytochrome p450 2B6 and 3A4 activity. Models of liver fibrosis have established that increases in YAP correlate with a decrease in the urea cycle [67]. Therefore, our data support the notion that YAP activity impairs the metabolic functions of hepatocytes. Previous studies have examined the mechanoregulation of hepatocytes, but many used serum, which is problematic for mechanotransduction studies as even low concentrations can provoke changes in cytoskeleton organisation [68,69], and influence YAP/TAZ nuclear localisation [70]. Here, our fully chemically defined differentiation protocol precludes a role for serum-mediated effects and instead highlights a role for physical cues alone driving YAP expression and hepatocyte differentiation.

In addition to stiffness, cell-matrix interactions influence integrin signalling, which have been found to regulate YAP/TAZ activity [71]. Integrin signalling is known to impact liver function, regeneration and disease progression [72], with ECM stiffness-stimulated integrin beta-1 signalling known to enhance nuclear translocation of YAP [73]. By reducing the concentration of RGD-motif-containing peptides in stiff gels, we were able to decrease the expression of YAP/TAZ target genes and improve hepatocyte differentiation. We also observed decreased *ITGB1* and *ITGB3* expression on soft substrates. Taken together, these data suggest that impaired hepatic function during fibrosis might result from increased integrin signalling [74]. However, when we reduced the concentration of RGD in soft hydrogels, differentiation was impaired. This suggests an interplay between substrate stiffness and RGD-mediated adhesion and that optimal conditions for both are required for effective differentiation.

hPSC-Heps can be generated that closely resemble PHH rather than fetal liver cells [75]. However, PHH rapidly dedifferentiate when placed in 2D culture [76] biasing direct comparison of metabolic functions. Albumin is the most widely used surrogate marker for hepatocyte functionality, and we have previously demonstrated that albumin protein expression correlated with *in vitro* functionality of both PHH and hPSC-Heps [5]. Importantly for future therapeutic applications, the level of secreted albumin we have reported for hPSC-Heps cultured on SOFT PEG (~7000 ng/million cells/day) is greater than what has been reported for expanded PHH [77–81], and higher than any report of which we are aware [77], confirming the power of our system to create functional cells.

As cellular therapies often require delivery within biomaterials, we also explored the impact of 3D hydrogel physical cues on encapsulated hPSC-Heps. We found that albumin production was lower in stiff 3D hydrogels compared to soft. Moreover, we report lower alpha-fetoprotein production in hPSC-Heps in 3D compared to 2D. These findings suggest that 3D soft culture could further improve hepatocyte differentiation and functionality. However, unlike on 2D substrates, in 3D culture, secreted proteins must diffuse out of hydrogels to be detectable in culture supernatants, a process that might be inhibited by the polymer network. Using mathematical models and experimental measurements, we have previously shown that the diffusion of molecules smaller than 70 kDa is comparable between 10% and 2.5% hydrogels [38]. This is because diffusion is only significantly impacted by polymer concentration when the solute size approaches that of the mesh network size. Here, as albumin (~5.5 nm [82]) and similarly sized alpha-fetoprotein [83] are much smaller than the predicted size of the mesh (10%: 6.43 nm; 2.5%: 8.41 nm), it is unlikely that hydrogel stiffness impacted these findings.

Here, we have shown that a material that mimics characteristics of the native liver niche, such as its stiffness, and provides a defined concentration of RGD-motif-containing peptides for cellular adhesion, improves the differentiation and function of hPSC-Heps compared to cells differentiated under conventional culture conditions. Additionally, we demonstrated advantages over alginate, which has been used clinically to delivery PHH into patients [84]. Building on our efforts to control biomaterial properties to enhance hPSC-Hep differentiation, technologies such as 3D printing using co-cultures may further allow for optimisation of hPSC-Heps differentiation. To date, there is no established medical intervention that utilises hPSC-derived therapeutics. However, with the generation and validation of cGMP-compliant cells, the development of robust fully defined, xeno-free differentiation protocols, and advances in fabricating synthetic materials that promote hepatocyte differentiation, it has become considerably easier to foresee a future where hPSC-Heps will be used as a curative intervention in patients with liver disease.

Credit author statement

Samuel J.I. Blackford: Conceptualization; Methodology; Investigation; Formal Analysis; Visualization; Writing – Original Draft; Writing – Review & Editing, Tracy T.L. Yu: Methodology; Investigation; Resources, Michael D.A. Norman: Investigation; Formal Analysis, Adam M. Syanda: Investigation, Michail Manolakakis: Investigation; Formal Analysis, Dariusz Lachowski: Investigation; Formal Analysis; Visualization, Ziqian Yan: Investigation, Yunzhe Guo: Resources, Elena Garitta: Investigation, Federica Riccio: Investigation, Geraldine M. Jowett: Investigation, Soon Seng Ng: Investigation, Santiago Vernia: Investigation; Formal Analysis, Armando E. del Río Hernández: Supervision; Resources, Eileen Gentleman: Conceptualization; Supervision; Writing – Original Draft; Writing – Review & Editing; Funding Acquisition, S. Tamir Rashid: Conceptualization; Supervision; Writing – Review & Editing; Funding Acquisition.

Funding

Guy's and St Thomas' NHS Foundation Trust Biomedical Research Centre (GSTT BRC) Ph.D. award: SJIB.

Biotechnology and Biological Sciences Research Council (BBSRC) studentship: MDAN.

The Rosetrees Trust: EG and YG.

Wellcome Trust Ph.D studentship: FR and GMJ.

King's College London Post-graduate Research International Studentship: ZY.

MRC Clinician Scientist Award MGSBACR: STR.

Declaration of competing interest

The authors declare the following financial interests/personal relationships which may be considered as potential competing interests:

S.T.R. is a scientific founder, shareholder, and consultant for DefiniGen, Ltd. The other authors indicated no potential conflicts of interest relevant to the study presented here.

Data availability

Data will be made available on request.

Acknowledgments

This research was funded/supported by the National Institute for Health Research (NIHR) Biomedical Research Centre based at Guy's and St Thomas' NHS Foundation Trust and King's College London and/or the NIHR Clinical Research Facility. The views expressed are those of the author(s) and not necessarily those of the NHS, the NIHR or the Department of Health and Social Care.

We acknowledge Cell and Gene Therapy Catapult (London, UK) and Dr. Ricardo Baptista for the generation and provision of the CGT-RCiB-10 hiPSC line. LiPSC-GR1.1 was supported by the NIH Common Fund Regenerative Medicine Generation of the GMP Program, and reported in Stem Cell Reports. The NIH Common Fund and the National Center for Advancing Translational Sciences (NCATS) are joint stewards of the LiPSC-GR1.1 resource.

Appendix A. Supplementary data

Supplementary data to this article can be found online at https://doi.org/10.1016/j.biomaterials.2022.121982.

References

[1] S.A. Gonzalez, E.B. Keeffe, Chronic viral hepatitis: epidemiology, molecular biology, and antiviral therapy, Front. Biosci. 16 (2011) 225–250, https://doi.org/10.2741/3685.

[2] V. Iansante, R.R. Mitry, C. Filippi, E. Fitzpatrick, A. Dhawan, Human hepatocyte transplantation for liver disease: current status and future perspectives, Pediatr. Res. 83 (2017) 232–240, https://doi.org/10.1038/pr.2017.284.

[3] P. Godoy, W. Schmidt-Heck, K. Natarajan, B. Lucendo-Villarin, D. Szkolnicka, A. Asplund, P. Björquist, A. Widera, R. Stöber, G. Campos, S. Hammad, A. Sachinidis, U. Chaudhari, G. Damm, T.S. Weiss, A. Nüssler, J. Synnergren, K. Edlund, B. Küppers-Munther, D.C. Hay, J.G. Hengstler, Gene networks and transcription factor motifs defining the differentiation of stem cells into hepatocyte-like cells, J. Hepatol. 63 (2015) 934–942, https://doi.org/10.1016/j.jhep.2015.05.013.

[4] M. Baxter, S. Withey, S. Harrison, C.P. Segeritz, F. Zhang, R. Atkinson-Dell, C. Rowe, D.T. Gerrard, R. Sison-Young, R. Jenkins, J. Henry, A.A. Berry, L. Mohamet, M. Best, S.W. Fenwick, H. Malik, N.R. Kitteringham, C.E. Goldring, K. Piper Hanley, L. Vallier, N.A. Hanley, Phenotypic and functional analyses show stem cell-derived hepatocyte-like cells better mimic fetal rather than adult hepatocytes, J. Hepatol. 62 (2015) 581–589, https://doi.org/10.1016/j.jhep.2014.10.016.

[5] J. Ong, M.P. Serra, J. Segal, A.-M. Cujba, S.S. Ng, R. Butler, V. Millar, S. Hatch, S. Zimri, H. Koike, K. Chan, A. Bonham, M. Walk, T. Voss, N. Heaton, R. Mitry, A. Dhawan, D. Ebner, D. Danovi, H. Nakauchi, S.T. Rashid, Imaging-based screen identifies laminin 411 as a physiologically relevant niche factor with importance for i-Hep applications, Stem Cell Rep. 10 (2018) 693–702, https://doi.org/10.1016/j.stemcr.2018.01.025.

[6] K. Sekine, S. Ogawa, S. Tsuzuki, T. Kobayashi, K. Ikeda, N. Nakanishi, K. Takeuchi, E. Kanai, Y. Otake, S. Okamoto, T. Kobayashi, T. Takebe, H. Taniguchi, Generation of human induced pluripotent stem cell-derived liver buds with chemically defined and animal origin-free media, Sci. Rep. 10 (2020), 17937, https://doi.org/10.1038/s41598-020-73908-1.

[7] A. Asai, E. Aihara, C. Watson, R. Mourya, T. Mizuochi, P. Shivakumar, K. Phelan, C. Mayhew, M. Helmrath, T. Takebe, J. Wells, J.A. Bezerra, Paracrine Signals Regulate Human Liver Organoid Maturation from Induced Pluripotent Stem Cells, vol. 144, Development, Cambridge, 2017, pp. 1056–1064, https://doi.org/10.1242/dev.142794.

[8] G. Zhao, J. Cui, Q. Qin, J. Zhang, L. Liu, S. Deng, C. Wu, M. Yang, S. Li, C. Wang, Mechanical stiffness of liver tissues in relation to integrin β1 expression may influence the development of hepatic cirrhosis and hepatocellular carcinoma, J. Surg. Oncol. 102 (2010) 482–489, https://doi.org/10.1002/jso.21613.

[9] T. Speicher, B. Siegenthaler, R.L. Bogorad, R. Ruppert, T. Petzold, S. Padrissa-Altes, M. Bachofner, D.G. Anderson, V. Koteliansky, R. Fässler, S. Werner, Knockdown and knockout of β1-integrin in hepatocytes impairs liver regeneration through inhibition of growth factor signalling, Nat. Commun. 5 (2014), https://doi.org/10.1038/ncomms4862.

[10] G. Patman, Liver: loss of integrin β1 impairs liver regeneration and HCC progression, Nat. Rev. Gastroenterol. Hepatol. 11 (2014) 392, https://doi.org/10.1038/nrgastro.2014.83.

[11] F. Calvo, N. Ege, A. Grande-Garcia, S. Hooper, R.P. Jenkins, S.I. Chaudhry, K. Harrington, P. Williamson, E. Moeendarbary, G. Charras, E. Sahai, Mechanotransduction and YAP-dependent matrix remodelling is required for the generation and maintenance of cancer-associated fibroblasts, Nat. Cell Biol. 15 (2013) 637–646, https://doi.org/10.1038/ncb2756.

[12] P. Chen, Q. Luo, C. Huang, Q. Gao, L. Li, J. Chen, B. Chen, W. Liu, W. Zeng, Z. Chen, Pathogenesis of non-alcoholic fatty liver disease mediated by YAP, Hepatol Int 12 (2018) 26–36, https://doi.org/10.1007/s12072-017-9841-y.

[13] D.H. Lee, J.O. Park, T.S. Kim, S.K. Kim, T.H. Kim, M.C. Kim, G.S. Park, J.H. Kim, S. Kuninaka, E.N. Olson, H. Saya, S.Y. Kim, H. Lee, D.S. Lim, LATS-YAP/TAZ controls lineage specification by regulating TGFβ signaling and Hnf4α expression during liver development, Nat. Commun. 7 (2016), https://doi.org/10.1038/ncomms11961.

[14] D. Yimlamai, C. Christodoulou, G.G. Galli, K. Yanger, B. Pepe-Mooney, B. Gurung, K. Shrestha, P. Cahan, B.Z. Stanger, F.D. Camargo, Hippo pathway activity influences liver cell fate, Cell 157 (2014) 1324–1338, https://doi.org/10.1016/j.cell.2014.03.060.

[15] L. Liu, G.R. Yannam, T. Nishikawa, T. Yamamoto, H. Basma, R. Ito, M. Nagaya, J. Dutta-Moscato, D.B. Stolz, F. Duan, K.H. Kaestner, Y. Vodovotz, A. Soto-Gutierrez, I.J. Fox, The microenvironment in hepatocyte regeneration and function in rats with advanced cirrhosis, Hepatology 55 (2012) 1529–1539, https://doi.org/10.1002/hep.24815.

[16] E.J. Semler, P.A. Lancin, A. Dasgupta, P.v. Moghe, Engineering hepatocellular morphogenesis and function via ligand-presenting hydrogels with graded mechanical compliance, Biotechnol. Bioeng. 89 (2005), https://doi.org/10.1002/bit.20328.

[17] E. Ruoslahti, Fibronectin and its receptors, Annu. Rev. Biochem. 57 (1988) 375–413, https://doi.org/10.1146/annurev.bi.57.070188.002111.

[18] D. MacPherson, Y. Bram, J. Park, R.E. Schwartz, Peptide-based scaffolds for the culture and maintenance of primary human hepatocytes, Sci. Rep. 11 (2021), https://doi.org/10.1038/s41598-021-86016-5.

[19] G.G.M. Pinkse, M.P. Voorhoeve, M. Noteborn, O.T. Terpstra, J.A. Bruijn, E. de Heer, Hepatocyte survival depends on β1-integrin-mediated attachment of hepatocytes to hepatic extracellular matrix, Liver Int. 24 (2004), https://doi.org/10.1111/j.1478-3231.2004.0914.x.

[20] J. You, S.-A. Park, D.-S. Shin, D. Patel, V.K. Raghunathan, M. Kim, C.J. Murphy, G. Tae, A. Revzin, Characterizing the effects of Heparin gel stiffness on function of primary hepatocytes, Tissue Eng. 19 (2013) 2655–2663, https://doi.org/10.1089/ten.tea.2012.0681.

[21] S.S. Desai, J.C. Tung, V.X. Zhou, J.P. Grenert, Y. Malato, M. Rezvani, R. Español-Suñer, H. Willenbring, V.M. Weaver, T.T. Chang, Physiological ranges of matrix rigidity modulate primary mouse hepatocyte function in part through hepatocyte nuclear factor 4 alpha, Hepatology 64 (2016) 261–275, https://doi.org/10.1002/hep.28450.

[22] H.J. Lee, M.J. Son, J. Ahn, S.J. Oh, M. Lee, A. Kim, Y.J. Jeung, H.G. Kim, M. Won, J.H. Lim, N.S. Kim, C.R. Jung, K.S. Chung, Elasticity-based development of functionally enhanced multicellular 3D liver encapsulated in hybrid hydrogel, Acta Biomater. 64 (2017) 67–79, https://doi.org/10.1016/j.actbio.2017.09.041.

[23] V. Natarajan, Y. Moeun, S. Kidambi, Exploring interactions between primary hepatocytes and non-parenchymal cells on physiological and pathological liver stiffness, Biology 10 (2021), https://doi.org/10.3390/biology10050408.

[24] E. Miller, J. Yang, M. Deran, C. Wu, A.I. Su, G.M.C. Bonamy, J. Liu, E.C. Peters, X. Wu, Identification of serum-derived sphingosine-1-phosphate as a small molecule regulator of YAP, Chem. Biol. 19 (2012) 955–962, https://doi.org/10.1016/j.chembiol.2012.07.005.

[25] M.D. Pierschbacher, E. Ruoslahti, Cell attachment activity of fibronectin can be duplicated by small synthetic fragments of the molecule, Nature 309 (1984), https://doi.org/10.1038/309030a0.

[26] G.M. Jowett, M.D.A. Norman, T.T.L. Yu, P. Rosell Arévalo, D. Hoogland, S.T. Lust, E. Read, E. Hamrud, N.J. Walters, U. Niazi, M.W.H. Chung, D. Marciano, O. S. Omer, T. Zabinski, D. Danovi, G.M. Lord, J. Hilborn, N.D. Evans, C.A. Dreiss, L. Bozec, O.P. Oommen, C.D. Lorenz, R.M.P. da Silva, J.F. Neves, E. Gentleman, ILC1 drive intestinal epithelial and matrix remodelling, Nat. Mater. 20 (2021) 250–259, https://doi.org/10.1038/s41563-020-0783-8.

[27] Q. Wei, S. Wang, F. Han, H. Wang, W. Zhang, Q. Yu, C. Liu, L. Ding, J. Wang, L. Yu, C. Zhu, B. Li, Cellular modulation by the mechanical cues from biomaterials for

tissue engineering, Biomaterials Translational 2 (2021) 323–342, https://doi.org/10.12336/biomatertransl.2021.04.001.
[28] N.J. Walters, E. Gentleman, Evolving insights in cell-matrix interactions: elucidating how non-soluble properties of the extracellular niche direct stem cell fate, Acta Biomater. 11 (2015) 3–16, https://doi.org/10.1016/j.actbio.2014.09.038.
[29] D.A. Foyt, M.D.A. Norman, T.T.L. Yu, E. Gentleman, Exploiting advanced hydrogel technologies to address key challenges in regenerative medicine, Adv Healthc Mater 7 (2018), https://doi.org/10.1002/adhm.201700939.
[30] M.D.A. Norman, S.A. Ferreira, G.M. Jowett, L. Bozec, E. Gentleman, Measuring the elastic modulus of soft culture surfaces and three-dimensional hydrogels using atomic force microscopy, Nat. Protoc. 16 (2021) 2418–2449, https://doi.org/10.1038/s41596-021-00495-4.
[31] L. Martinez, R. Andrade, E.G. Birgin, J.M. Martínez, PACKMOL: a package for building initial configurations for molecular dynamics simulations, J. Comput. Chem. 30 (2009) 2157–2164, https://doi.org/10.1002/jcc.21224.
[32] S.J.I. Blackford, S.S. Ng, J.M. Segal, A.J.F. King, A.L. Austin, D. Kent, J. Moore, M. Sheldon, D. Ilic, A. Dhawan, R.R. Mitry, S.T. Rashid, Validation of current good manufacturing practice compliant human pluripotent stem cell-derived hepatocytes for cell-based therapy, Stem Cells Transl Med 8 (2019) 124–137, https://doi.org/10.1002/sctm.18-0084.
[33] A.M. Jobbins, N. Haberman, N. Artigas, C. Amourda, H.A.B. Paterson, S. Yu, S.J. I. Blackford, A. Montoya, M. Dore, Y.F. Wang, A. Sardini, I. Cebola, J. Zuber, S. T. Rashid, B. Lenhard, S. Vernia, Dysregulated RNA polyadenylation contributes to metabolic impairment in non-alcoholic fatty liver disease, Nucleic Acids Res. 50 (2022), https://doi.org/10.1093/nar/gkac165.
[34] D. Lachowski, E. Cortes, C. Matellan, A. Rice, D.A. Lee, S.D. Thorpe, A.E. del Río, G. Hernández, Protein-Coupled estrogen receptor regulates actin cytoskeleton dynamics to impair cell polarization, Front. Cell Dev. Biol. 8 (2020), https://doi.org/10.3389/fcell.2020.592628.
[35] J. Schindelin, I. Arganda-Carreras, E. Frise, V. Kaynig, M. Longair, T. Pietzsch, S. Preibisch, C. Rueden, S. Saalfeld, B. Schmid, J.Y. Tinevez, D.J. White, V. Hartenstein, K. Eliceiri, P. Tomancak, A. Cardona, Fiji: an open-source platform for biological-image analysis, Nat. Methods 9 (2012), https://doi.org/10.1038/nmeth.2019.
[36] O.A. Lozoya, E. Wauthier, R.A. Turner, C. Barbier, G.D. Prestwich, F. Guilak, R. Superfine, S.R. Lubkin, L.M. Reid, Regulation of hepatic stem/progenitor phenotype by microenvironment stiffness in hydrogel models of the human liver stem cell niche, Biomaterials 32 (2011) 7389–7402, https://doi.org/10.1016/j.biomaterials.2011.06.042.
[37] S.S. Ng, K. Saeb-Parsy, S.J.I. Blackford, J.M. Segal, M.P. Serra, M. Horcas-Lopez, D. Y. No, S. Mastoridis, W. Jassem, C.W. Frank, N.J. Cho, H. Nakauchi, J.S. Glenn, S. T. Rashid, Human iPS derived progenitors bioengineered into liver organoids using an inverted colloidal crystal poly (ethylene glycol) scaffold, Biomaterials 182 (2018) 299–311, https://doi.org/10.1016/j.biomaterials.2018.07.043.
[38] S.T. Lust, D. Hoogland, M.D.A. Norman, C. Kerins, J. Omar, G.M. Jowett, T.T.L. Yu, Z. Yan, J.Z. Xu, D. Marciano, R.M.P. da Silva, C.A. Dreiss, P. Lamata, R.J. Shipley, E. Gentleman, Selectively cross-linked tetra-PEG hydrogels provide control over mechanical strength with minimal impact on diffusivity, ACS Biomater. Sci. Eng. 7 (2021), https://doi.org/10.1021/acsbiomaterials.0c01723.
[39] E. Nguyen-Khac, D. Chatelain, B. Tramier, C. Decrombecque, B. Robert, J.P. Joly, M. Brevet, P. Grignon, S. Lion, L. le Page, J.L. Dupas, Assessment of asymptomatic liver fibrosis in alcoholic patients using fibroscan: prospective comparison with seven non-invasive laboratory tests, Aliment. Pharmacol. Ther. 28 (2008) 1188–1198, https://doi.org/10.1111/j.1365-2036.2008.03831.x.
[40] G. Mazza, W. Al-Akkad, A. Telese, L. Longato, L. Urbani, B. Robinson, A. Hall, K. Kong, L. Frenguelli, G. Marrone, O. Willacy, M. Shaeri, A. Burns, M. Malago, J. Gilbertson, N. Rendell, K. Moore, D. Hughes, I. Notingher, G. Jell, A. del Rio Hernandez, P. de Coppi, K. Rombouts, M. Pinzani, Rapid production of human liver scaffolds for functional tissue engineering by high shear stress oscillation-decellularization, Sci. Rep. 7 (2017), https://doi.org/10.1038/s41598-017-05134-1.
[41] N. Mittal, F. Tasnim, C. Yue, Y. Qu, D. Phan, Y. Choudhury, M.H. Tan, H. Yu, Substrate stiffness modulates the maturation of human pluripotent stem-cell-derived hepatocytes, ACS Biomater. Sci. Eng. 2 (2016) 1649–1657, https://doi.org/10.1021/acsbiomaterials.6b00475.
[42] I. Kyrmizi, P. Hatzis, N. Katrakili, F. Tronche, F.J. Gonzalez, I. Talianidis, Plasticity and expanding complexity of the hepatic transcription factor network during liver development, Genes Dev. 20 (2006) 2293–2305, https://doi.org/10.1101/gad.390906.
[43] Y. Hu, D.J. Shin, H. Pan, Z. Lin, J.M. Dreyfuss, F.D. Camargo, J. Miao, S. B. Biddinger, YAP suppresses gluconeogenic gene expression through PGC1α, Hepatology 66 (2017) 2029–2041, https://doi.org/10.1002/hep.29373.
[44] S.Y. Choi, H. Bae, S.H. Jeong, I. Park, H. Cho, S.P. Hong, D.H. Lee, C. kun Lee, J. S. Park, S.H. Suh, J. Choi, M.J. Yang, J.Y. Jang, L. Onder, J.H. Moon, H.S. Jeong, R. H. Adams, J.M. Kim, B. Ludewig, J.H. Song, D.S. Lim, G.Y. Koh, YAP/TAZ direct commitment and maturation of lymph node fibroblastic reticular cells, Nat. Commun. 11 (2020) 519, https://doi.org/10.1038/s41467-020-14293-1.
[45] L. Yang, S. Inokuchi, Y.S. Roh, J. Song, R. Loomba, E.J. Park, E. Seki, Transforming growth factor-β signaling in hepatocytes promotes hepatic fibrosis and carcinogenesis in mice with hepatocyte-specific deletion of TAK1, Gastroenterology 144 (2013), https://doi.org/10.1053/j.gastro.2013.01.056.
[46] A. Dropmann, T. Dediulia, K. Breitkopf-Heinlein, H. Korhonen, M. Janicot, S. N. Weber, M. Thomas, A. Piiper, E. Bertran, I. Fabregat, K. Abshagen, J. Hess, P. Angel, C. Coulouarn, D. Steven, N.M. Meindl-Beinker, TGF-β1 and TGF-β2 abundance in liver diseases of mice and men, Oncotarget 7 (2016) 19499–19518, https://doi.org/10.18632/oncotarget.6967.
[47] S.H. Oh, M. Swiderska-Syn, M.L. Jewell, R.T. Premont, A.M. Diehl, Liver regeneration requires Yap1-TGFβ-dependent epithelial-mesenchymal transition in hepatocytes, J. Hepatol. 69 (2018), https://doi.org/10.1016/j.jhep.2018.05.008.
[48] R.O. Hynes, Integrins: bidirectional, allosteric signaling machines, Cell 110 (2002) 673–687, https://doi.org/10.1016/s0092-8674(02)00971-6.
[49] A. Couvelard, A.-F. Bringuier, M.-C. Dauge, M. Nejjari, E. Darai, J.-L. Benifla, G. Feldmann, D. Henin, J.-Y. Scoazec, Expression of integrins during liver organogenesis in humans, Hepatology 27 (1998) 839–847, https://doi.org/10.1002/hep.510270328.
[50] Y. Liu-Chittenden, B. Huang, J.S. Shim, Q. Chen, S.J. Lee, R.A. Anders, J.O. Liu, D. Pan, Genetic and pharmacological disruption of the TEAD-YAP complex suppresses the oncogenic activity of YAP, Genes Dev. 26 (2012) 1300–1305, https://doi.org/10.1101/gad.192856.112.
[51] P. Sun, G. Zhang, X. Su, C. Jin, B. Yu, X. Yu, Z. Lv, H. Ma, M. Zhang, W. Wei, W. Li, Maintenance of primary hepatocyte functions in vitro by inhibiting mechanical tension-induced YAP activation, Cell Rep. 29 (2019), https://doi.org/10.1016/j.celrep.2019.10.128.
[52] A.M. Syanda, V.I. Kringstad, S.J.I. Blackford, J.S. Kjesbu, S.S. Ng, L. Ma, F. Xiao, A. E. Coron, A.M.A. Rokstad, S. Modi, S.T. Rashid, B.L. Strand, Sulfated alginate reduces pericapsular fibrotic overgrowth on encapsulated cGMP-compliant hPSC-hepatocytes in mice, Front. Bioeng. Biotechnol. 9 (2022), https://doi.org/10.3389/fbioe.2021.816542.
[53] J.H. Lee, D.H. Lee, S. Lee, C.H. David Kwon, J.N. Ryu, J.K. Noh, I.K. Jang, H. J. Park, H.H. Yoon, J.K. Park, Y.J. Kim, S.K. Kim, S.K. Lee, Functional evaluation of a bioartificial liver support system using immobilized hepatocyte spheroids in a porcine model of acute liver failure, Sci. Rep. 7 (2017), https://doi.org/10.1038/s41598-017-03424-2.
[54] Z. Machaidze, H. Yeh, L. Wei, C. Schuetz, M. Carvello, A. Sgroi, R.N. Smith, H. J. Schuurman, D.H. Sachs, P. Morel, J.F. Markmann, L.H. Bühler, Testing of microencapsulated porcine hepatocytes in a new model of fulminant liver failure in baboons, Xenotransplantation 24 (2017), https://doi.org/10.1111/xen.12297.
[55] A. Dhawan, N. Chaijitraruch, E. Fitzpatrick, S. Bansal, C. Filippi, S.C. Lehec, N. D. Heaton, P. Kane, A. Verma, R.D. Hughes, R.R. Mitry, Alginate microencapsulated human hepatocytes for the treatment of acute liver failure in children, J. Hepatol. 72 (2020), https://doi.org/10.1016/j.jhep.2019.12.002.
[56] J.D. Weaver, D.M. Headen, M.M. Coronel, M.D. Hunckler, H. Shirwan, A.J. García, Synthetic poly(ethylene glycol)-based microfluidic islet encapsulation reduces graft volume for delivery to highly vascularized and retrievable transplant site, Am. J. Transplant. 19 (2019), https://doi.org/10.1111/ajt.15168.
[57] J. Petzold, E. Gentleman, Intrinsic mechanical cues and their impact on stem cells and embryogenesis, Front. Cell Dev. Biol. 9 (2021), https://doi.org/10.3389/fcell.2021.761871.
[58] K. Cameron, B. Lucendo-Villarin, D. Szkolnicka, D.C. Hay, Serum-free directed differentiation of human embryonic stem cells to hepatocytes, in: Protocols in in Vitro Hepatocyte Research, 2015, pp. 105–111, https://doi.org/10.1007/978-1-4939-2074-7_7.
[59] N.R.F. Hannan, C.-P. Segeritz, T. Touboul, L. Vallier, Production of hepatocyte-like cells from human pluripotent stem cells, Nat. Protoc. 8 (2013) 430–437, https://doi.org/10.1038/nprot.2012.153.
[60] C. Rodríguez-Antona, M.T. Donato, A. Boobis, R.J. Edwards, P.S. Watts, J. v. Castell, M.J. Gómez-Lechón, Cytochrome P450 expression in human hepatocytes and hepatoma cell lines: molecular mechanisms that determine lower expression in cultured cells, Xenobiotica 32 (2002) 505–520, https://doi.org/10.1080/00498250210128675.
[61] M. Kacevska, G.R. Robertson, S.J. Clarke, C. Liddle, Inflammation and CYP3A4-mediated drug metabolism in advanced cancer: impact and implications for chemotherapeutic drug dosing, Expet Opin. Drug Metabol. Toxicol. 4 (2008) 137–149, https://doi.org/10.1517/17425255.4.2.137.
[62] U.M. Zanger, M. Schwab, Cytochrome P450 enzymes in drug metabolism: regulation of gene expression, enzyme activities, and impact of genetic variation, Pharmacol. Ther. 138 (2013) 103–141, https://doi.org/10.1016/j.pharmthera.2012.12.007.
[63] D. Chen, H. Zhang, X. Zhang, X. Sun, Q. Qin, Y. Hou, M. Jia, Y. Chen, Roles of Yes-associated protein and transcriptional coactivator with PDZ-binding motif in non-neoplastic liver diseases, Biomed. Pharmacother. 151 (2022), 113166, https://doi.org/10.1016/j.biopha.2022.113166.
[64] Z. Chen, N. Tang, X. Wang, Y. Chen, The activity of the carbamoyl phosphate synthase 1 promoter in human liver-derived cells is dependent on hepatocyte nuclear factor 3-beta, J. Cell Mol. Med. 21 (2017), https://doi.org/10.1111/jcmm.13123.
[65] F.X. Yu, B. Zhao, N. Panupinthu, J.L. Jewell, I. Lian, L.H. Wang, J. Zhao, H. Yuan, K. Tumaneng, H. Li, X.D. Fu, G.B. Mills, K.L. Guan, Regulation of the Hippo-YAP pathway by G-protein-coupled receptor signaling, Cell 150 (2012) 780–791, https://doi.org/10.1016/j.cell.2012.06.037.
[66] F.X. Yu, Y. Zhang, H.W. Park, J.L. Jewell, Q. Chen, Y. Deng, D. Pan, S.S. Taylor, Z. C. Lai, K.L. Guan, Protein kinase A activates the Hippo pathway to modulate cell proliferation and differentiation, Genes Dev. 27 (2013) 1223–1232, https://doi.org/10.1101/gad.219402.113.
[67] T. Su, T. Bondar, X. Zhou, C. Zhang, H. He, R. Medzhitov, Two-signal Requirement for Growth-Promoting Function of Yap in Hepatocytes, Elife. 2015, 2015, https://doi.org/10.7554/eLife.02948.
[68] A.J. Ridley, A. Hall, The small GTP-binding protein rho regulates the assembly of focal adhesions and actin stress fibers in response to growth factors, Trends Cell Biol. 2 (1992) 324, https://doi.org/10.1016/0962-8924(92)90173-k.

[69] A.J. Ridley, H.F. Paterson, C.L. Johnston, D. Diekmann, A. Hall, The small GTP-binding protein rac regulates growth factor-induced membrane ruffling, Trends Cell Biol. 2 (1992) 324, https://doi.org/10.1016/0962-8924(92)90174-l.
[70] S. Pijuan-Galitó, C. Tamm, C. Annerén, Serum inter-α-inhibitor activates the yes tyrosine kinase and YAP/TEAD transcriptional complex in mouse embryonic stem cells, J. Biol. Chem. 289 (2014) 33492–33502, https://doi.org/10.1074/jbc.M114.580076.
[71] A. Elbediwy, Z.I. Vincent-Mistiaen, B. Spencer-Dene, R.K. Stone, S. Boeing, S. K. Wculek, J. Cordero, E.H. Tan, R. Ridgway, V.G. Brunton, E. Sahai, H. Gerhardt, A. Behrens, I. Malanchi, O.J. Sansom, B.J. Thompson, Integrin signalling regulates YAP and TAZ to control skin homeostasis, Development 143 (2016) 1674–1687, https://doi.org/10.1242/dev.133728.
[72] N. Martucci, G.K. Michalopoulos, W.M. Mars, Integrin linked kinase (ILK) and its role in liver pathobiology, Gene Expression The Journal of Liver Research 20 (2021), https://doi.org/10.3727/105221621X16113475275710.
[73] M. Passi, S. Zahler, Mechano-signaling aspects of hepatocellular carcinoma, J. Cancer 12 (2021), https://doi.org/10.7150/jca.60102.
[74] E. Patsenker, F. Stickel, Role of integrins in fibrosing liver diseases, Am. J. Physiol. Gastrointest. Liver Physiol. 301 (2011) 424–434, https://doi.org/10.1152/ajpgi.00050.2011.
[75] N. Ghosheh, B. Küppers-Munther, A. Asplund, C.X. Andersson, P. Björquist, T. B. Andersson, H. Carén, S. Simonsson, P. Sartipy, J. Synnergren, Human pluripotent stem cell-derived hepatocytes show higher transcriptional correlation with adult liver tissue than with fetal liver tissue, ACS Omega 5 (2020) 4816–4827, https://doi.org/10.1021/acsomega.9b03514.
[76] C.C. Bell, A.C.A. Dankers, V.M. Lauschke, R. Sison-Young, R. Jenkins, C. Rowe, C. E. Goldring, K. Park, S.L. Regan, T. Walker, C. Schofield, A. Baze, A.J. Foster, D. P. Williams, A.W.M. van de Ven, F. Jacobs, J. van Houdt, T. Lähteenmäki, J. Snoeys, S. Juhila, L. Richert, M. Ingelman-Sundberg, Comparison of hepatic 2D sandwich cultures and 3d spheroids for long-term toxicity applications: a multicenter study, Toxicol. Sci. 162 (2018), https://doi.org/10.1093/toxsci/kfx289.
[77] K. Zhang, L. Zhang, W. Liu, X. Ma, J. Cen, Z. Sun, C. Wang, S. Feng, Z. Zhang, L. Yue, L. Sun, Z. Zhu, X. Chen, A. Feng, J. Wu, Z. Jiang, P. Li, X. Cheng, D. Gao, L. Peng, L. Hui, Vitro expansion of primary human hepatocytes with efficient liver repopulation capacity, Cell Stem Cell 23 (2018), https://doi.org/10.1016/j.stem.2018.10.018.
[78] M. Cuvellier, S. Rose, F. Ezan, U. Jarry, H. de Oliveira, A. Bruyère, C. Drieu La Rochelle, V. Legagneux, S. Langouët, G. Baffet, In vitro long term differentiation and functionality of three-dimensional bioprinted primary human hepatocytes: application for in vivo engraftment, Biofabrication 14 (2022), 35021, https://doi.org/10.1088/1758-5090/ac7825.
[79] G.B. Fu, W.J. Huang, M. Zeng, X. Zhou, H.P. Wu, C.C. Liu, H. Wu, J. Weng, H. D. Zhang, Y.C. Cai, C. Ashton, M. Ding, D. Tang, B.H. Zhang, Y. Gao, W.F. Yu, B. Zhai, Z.Y. He, H.Y. Wang, H.X. Yan, Expansion and differentiation of human hepatocyte-derived liver progenitor-like cells and their use for the study of hepatotropic pathogens, Cell Res. 29 (2019), https://doi.org/10.1038/s41422-018-0103-x.
[80] C. Gu, M. Chai, J. Liu, H. Wang, W. Du, Y. Zhou, W.S. Tan, Expansion of transdifferentiated human hepatocytes in a serum-free microcarrier culture system, Dig. Dis. Sci. 65 (2020), https://doi.org/10.1007/s10620-019-05925-8.
[81] D.P. Collins, J.H. Hapke, R.N. Aravalli, C.J. Steer, Development of immortalized human hepatocyte-like hybrid cells by fusion of multi-lineage progenitor cells with primary hepatocytes, PLoS One 15 (2020), https://doi.org/10.1371/journal.pone.0234002.
[82] L.M. Karlsson, P. Tengvall, I. Lundström, H. Arwin, Penetration and loading of human serum albumin in porous silicon layers with different pore sizes and thicknesses, J. Colloid Interface Sci. 266 (2003), https://doi.org/10.1016/S0021-9797(03)00595-2.
[83] M. Irony-Tur-Sinai, N. Grigoriadis, D. Tsiantoulas, O. Touloumi, O. Abramsky, T. Brenner, Immunomodulation of EAE by alpha-fetoprotein involves elevation of immune cell apoptosis markers and the transcription factor FoxP3, J. Neurol. Sci. 279 (2009), https://doi.org/10.1016/j.jns.2008.12.014.
[84] P.J. McKiernan, R.H. Squires, Bridging transplantation with beads in paediatric acute liver failure, Nat. Rev. Gastroenterol. Hepatol. 17 (2020), https://doi.org/10.1038/s41575-020-0281-0.